THE JOURNAL OF BIOLOGICAL CHEMISTRY VOL. 283, NO. 42, pp. 28176–28189, October 17, 2008

The Ratio of Monomeric to Aggregated Forms of Aβ40 and Aβ42 Is an Important Determinant of Amyloid-β Aggregation, Fibrillogenesis, and Toxicity*[S]

Received for publication, April 24, 2008, and in revised form, August 6, 2008 Published, JBC Papers in Press, August 11, 2008, DOI 10.1074/jbc.M803159200

Asad Jan[‡], Ozgun Gokce[§], Ruth Luthi-Carter[§], and Hilal A. Lashuel[‡1]

From the [‡]Laboratory of Molecular Neurobiology and Neuroproteomics and [§]Laboratory of Functional Neurogenomics, Brain Mind Institute, Ecole Polytechnique Fédérale de Lausanne, CH-1015 Lausanne, Switzerland

Aggregation and fibril formation of amyloid-β (Aβ) peptides Aβ40 and Aβ42 are central events in the pathogenesis of Alzheimer disease. Previous studies have established the ratio of Aβ40 to Aβ42 as an important factor in determining the fibrillogenesis, toxicity, and pathological distribution of Aβ. To better understand the molecular basis underlying the pathologic consequences associated with alterations in the ratio of Aβ40 to Aβ42, we probed the concentration- and ratio-dependent interactions between well defined states of the two peptides at different stages of aggregation along the amyloid formation pathway. We report that monomeric Aβ40 alters the kinetic stability, solubility, and morphological properties of Aβ42 aggregates and prevents their conversion into mature fibrils. Aβ40, at approximately equimolar ratios (Aβ40/Aβ42 ~ 0.5–1), inhibits (>50%) fibril formation by monomeric Aβ42, whereas inhibition of protofibrillar Aβ42 fibrillogenesis is achieved at lower, substoichiometric ratios (Aβ40/Aβ42 ~ 0.1). The inhibitory effect of Aβ40 on Aβ42 fibrillogenesis is reversed by the introduction of excess Aβ42 monomer. Additionally, monomeric Aβ42 and Aβ40 are constantly recycled and compete for binding to the ends of protofibrillar and fibrillar Aβ aggregates. Whereas the fibrillogenesis of both monomeric species can be seeded by fibrils composed of either peptide, Aβ42 protofibrils selectively seed the fibrillogenesis of monomeric Aβ42 but not monomeric Aβ40. Finally, we also show that the amyloidogenic propensities of different individual and mixed Aβ species correlates with their relative neuronal toxicities. These findings, which highlight specific points in the amyloid peptide equilibrium that are highly sensitive to the ratio of Aβ40 to Aβ42, carry important implications for the pathogenesis and current therapeutic strategies of Alzheimer disease.

Alzheimer disease is a progressive neurodegenerative disorder characterized by age-related accumulation of amyloid-β (Aβ)[2] proteins in the form of diffuse and neuritic plaques in regions of the brain that are affected by the disease (1–4). The discovery of Aβ fibrils as principal constituents of amyloid plaques led to the emergence of the amyloid hypothesis, which implicates the aggregation of Aβ as the primary trigger for a cascade of pathogenic events culminating in neurodegeneration and development of AD (1, 5–7). Aβ proteins are produced in neuronal and non-neuronal cells as a result of sequential proteolytic cleavage of the type I transmembrane amyloid precursor protein (APP) by β- and γ-secretases (8–12). Depending on the site of APP cleavage by γ-secretase, Aβ proteins of various chain lengths are generated (13–16). The predominant Aβ species in human plasma and CSF, as well as in conditioned media of APP-expressing cells, is Aβ40 (~90%) followed by Aβ42 (~10%). Despite the preponderance of Aβ40, *in vivo* studies reveal that Aβ42 is a major constituent of amyloid plaques and suggest that Aβ42 aggregation plays a critical role in the initiation of plaque formation and AD pathogenesis (17–20). *In vitro*, Aβ42 exhibits lower solubility and has the propensity to form protofibrils and fibrillar aggregates at lower concentrations and higher rates than Aβ40 or other Aβ variants (21–23). Aβ42 aggregates (protofibrils and fibrils) have also been reported to be more toxic to cultured neurons than Aβ40 aggregates (24, 25).

Although the majority of late-onset AD cases occur sporadically, genetic mutations in APP or subunits of γ-secretase (presenilins PS1 or PS2) account for a significant proportion of early-onset familial AD (FAD) cases (26, 27). Animal models and *in vitro* cell culture studies have shown that, in most instances, FAD mutations enhance total Aβ production, promote its aggregation and brain deposition, and/or alter the Aβ40/Aβ42 ratio in favor of Aβ42 production (28–30). Recent studies in human subjects also highlight the importance of Aβ40/Aβ42 ratio, rather than the total concentration of Aβ, as an important biomarker for AD progression and disease severity (31–33). To evaluate the consequences of altering the ratio Aβ40/Aβ42, several groups have investigated the effect of co-expressing the two Aβ variants (Aβ40 and Aβ42) or altering the expression level of one or the other variant in cellular and animal models of AD. These studies and other studies in human patients demon-

* This work was supported by the Swiss Federal Institute of Technology Lausanne (all investigators) and Grant 310000-110027 from the Swiss National Science Foundation (to H. L. A. and A. J.). The costs of publication of this article were defrayed in part by the payment of page charges. This article must therefore be hereby marked "*advertisement*" in accordance with 18 U.S.C. Section 1734 solely to indicate this fact.

[S] The on-line version of this article (available at http://www.jbc.org) contains supplemental Figs. 1–6.

[1] To whom correspondence should be addressed: Laboratory of Molecular Biology and Neuroproteomics, Brain Mind Inst., Ecole Polytechnique Fédérale de Lausanne (EPFL), CH-1015, Lausanne, Switzerland. Fax: 41-21-693-96-65; E-mail: hilal.lashuel@epfl.ch.

[2] The abbreviations used are: Aβ, amyloid-β; AD, Alzheimer disease; FAD, familial Alzheimer disease; APP, amyloid precursor protein; PF, protofibrillar; M, monomeric; F, fibrillar; SF, sonicated fibrils; SEC, size exclusion chromatography; ThT, thioflavin T; TEM, transmission electron microscopy; PBS, phosphate-buffered saline.

strate that the ratio of Aβ40 to Aβ42 is an important determinant of the distribution of amyloid pathology (*i.e.* parenchymal or vascular amyloid deposition) in the brains of patients with AD and transgenic AD mouse models (18, 34–37).

The molecular mechanisms by which changes in the Aβ40/Aβ42 ratio modulate the aggregation and toxicity of Aβ and influence the amyloid pathology distribution in the AD brain remain the subjects of considerable debate. Aβ40 inhibits fibril formation by Aβ42 (22, 38), and co-incubation of the two Aβ variants leads to formation of mixed prefibrillar aggregates *in vitro* (39). Aβ40 prevents Aβ42-induced neurotoxicity in cultured cells and *in vivo* (40), underscoring the regulatory effects of Aβ40/Aβ42 ratio on important events associated with Aβ aggregation and toxicity. More recently, Yan and Wang (41) used differential NMR isotope labeling to demonstrate that Aβ40 prevents aggregation of monomeric Aβ42 and is capable of being exchanged for Aβ42 monomer in Aβ42 aggregates.

In the present study, we determined the preferential effect of Aβ40 on the kinetic stability, solubility, and fibrillogenesis rate of specific aggregation states of Aβ42, including monomers, protofibrils, and fibrils. Additionally, we explored the dynamics of exchange between monomeric Aβ40 and Aβ42 at the end of protofibrils and fibrils formed by each peptide and determined the effect of these interactions on the aggregate growth and morphology *in vitro*. Finally, we examined the ability of Aβ42 fibrils and protofibrils to seed the aggregation of Aβ40 and vice versa by monitoring the seeding effects of homologous and heterologous sequence on the lag phase, elongation phase, and steady-state phase of fibril formation of monomeric Aβ40 and Aβ42. The specificity of interaction between Aβ40 and different Aβ42 aggregation states was validated by using Aβ40-1 (reverse) as a control peptide. The present work provides novel mechanistic and structural insights into the molecular mechanisms underlying the consequences associated with altered Aβ40/Aβ42 ratio. The implications of these findings for intervention strategies for AD are also discussed.

EXPERIMENTAL PROCEDURES

Chemicals and reagents of analytical grade were purchased from Sigma-Aldrich unless indicated otherwise. Best quality distilled water was used for preparation of buffers and solutions, which were filtered through 0.65-μm DVPP membranes (Millipore) before use.

Preparation of Protofibrillar and Monomeric Aβ

Aβ peptides 1-40, 1-42, and 40-1 were synthesized and purified by Dr. James I. Elliott at Yale University (New Haven, CT). Protofibrillar (PF) and monomeric (M) forms of Aβ were prepared according to the protocols described previously (42). Briefly, Aβ peptides were dissolved in 100% DMSO and adjusted to 1 mg/ml by adding distilled H_2O. The pH of the resultant solutions was adjusted with 2 M Tris base, pH 7.4. After centrifugation (8000 × *g* at 4 °C for 10 min) the supernatant was injected into a size exclusion chromatography column Superdex 75 HR 10/30 (GE Healthcare) that had been equilibrated previously with 10 mM Tris-HCl, pH 7.4. Peptides were fractionated at a flow rate of 0.5 ml/min and eluted in 1.5-column volumes. Aβ elution was monitored by UVabsorbance at three different wavelengths: 210, 254, and 280 nm. Under these conditions, Aβ42 eluted as two well separated peaks; one corresponding to the void volume of Superdex 75 containing Aβ protofibrils ($Aβ42_{PF}$) and the second peak corresponding to monomeric Aβ ($Aβ42_{M}$) (supplemental Fig. 1). Aβ40 and Aβ40-1 elute predominantly as single peaks corresponding to monomeric species (data not shown). The protein concentrations of the various Aβ fractions was estimated by UV absorbance at 280 nm in 10-mm path-length cuvettes using the theoretical molar extinction coefficient at 280 nm (1490 M^{-1} cm^{-1}) (43) and/or using the Micro BCA protein assay (Pierce) when needed.

Fibrillogenesis Studies

Co-incubation of Monomeric Aβ40 with Protofibrillar or Monomeric Aβ42—Monomeric and protofibrillar preparations of Aβ42 and Aβ40 obtained by size exclusion chromatography (SEC) were adjusted to a final concentration of 10–20 μM in 10 mM Tris-HCl, pH 7.4, and placed in a 37 °C incubator without agitation. For co-incubation studies, protofibrillar and monomeric Aβ42 fractions were mixed with monomeric Aβ40 at molar ratios ($Aβ42_{M}$:$Aβ40_{M}$) of 10:1, 10:5, and 10:10 (all concentrations in μM) and allowed to aggregate at 37 °C without agitation. Fibril formation and protein solubility were monitored by thioflavin T (ThT) binding assay, negative staining transmission electron microscopy (TEM), and analytical SEC as described below. In parallel, the specificity of Aβ40 interactions with Aβ42 was validated by co-incubation with the control peptide Aβ40-1.

Fibril Elongation Studies—To probe the effect of monomeric Aβ on the elongation and reassociation of Aβ42 fibrils, we first generated Aβ42 fibrils by incubating 10 μM monomeric Aβ42 ($Aβ42_{M}$) for 96 h. The fibrils were mechanically fragmented into smaller fibrillar structures (100–300 nm long) by ultrasonication on ice using a Vibra Cell™ instrument (Sonics Inc.) equipped with a 2-mm diameter microtip (20 × 5 s pulses; amplitude, 40%; output, 6 watts). The sonicated fibrils ($Aβ42_{SF}$) were incubated: (i) in isolation; (ii) with monomeric Aβ42 (10 μM); (iii) with monomeric Aβ40 (10 μM); or (iv) with a 1:1 mixture of monomeric Aβ42:40 (20 μM final Aβ concentration). Fibril elongation and reformation of mature Aβ fibrils was monitored by ThT fluorescence and TEM.

Seeding Polymerization Studies

Seeding the Fibrillogenesis of Monomeric Aβ (Aβ40 and Aβ42) with Fibrils Derived from Aβ40 and Aβ42—To probe the ability of Aβ42 fibrils to accelerate the fibrillogenesis of monomeric Aβ40 and vice versa, 20 μM monomeric Aβ (Aβ42 or Aβ40) was incubated with the following: (i) 10 μg/ml sonicated Aβ42 fibrils ($Aβ42_{SF}$, once); (ii) 20 μg/ml sonicated Aβ42 fibrils ($Aβ42_{SF}$, twice); (iii) 10 μg/ml sonicated Aβ40 fibrils ($Aβ40_{SF}$, once); and (iv) 20 μg/ml sonicated Aβ40 fibrils ($Aβ40_{SF}$, twice). The extent of fibril formation was determined by ThT fluorescence and TEM. ThT fluorescence data were normalized by subtracting the contribution from sonicated fibrils.

Seeding the Fibrillogenesis of Monomeric Aβ (Aβ40 and Aβ42) with Aβ42 Protofibrils—20 μM monomeric Aβ (Aβ40 or Aβ42) was co-incubated with different molar ratios of protofibrillar Aβ42 (monomeric Aβ:$Aβ42_{PF}$; 20:1, 20:2 and 20:4; all final concentrations in μM) and fibril formation was monitored by ThT fluorescence after subtracting the contribution from protofibrillar Aβ42. To probe the specificity of interactions between the monomeric and aggregated forms of Aβ42 and Aβ40, we also evaluated the capacity of sonicated fibrils and protofibrillar species of both peptides (Aβ40 and Aβ42) to seed the fibrillogenesis of Aβ40-1 (20 μM) in a similar fashion.

Thioflavin T Binding Assay

ThT binding assay was performed by mixing aliquots of 10–20 μM Aβ with 10–20 μM ThT dye (Aβ:ThT 1:1) and 50 mM glycine-NaOH, pH 8.5, in Nunc 384-well fluorescence plates (Fisher Scientific). ThT fluorescence of each sample was measured in an Analyst AD fluorometer (Molecular Devices) at excitation and emission wavelengths of 450 and 485 nm, respectively. The samples were analyzed in duplicates at selected time points.

Transmission Electron Microscopy

5 μl of sample was applied to carbon-coated Formvar 200 mesh grids (Electron Microscopy Sciences) and incubated at room temperature for 60 s. The grids were then washed sequentially by depositing 10-μl droplets of double distilled sterile water (2 times) followed by a 10-μl droplet of fresh 2% (w/v) uranyl acetate, which remained on the grid for 30 s. After each step, the excess solution was blotted with Whatman filter paper, and the grids were vacuum-dried from the edges. The samples were analyzed using a Philips CM-10 TEM microscope operated at 100 kV acceleration voltage.

Analytical Size Exclusion Chromatography

Analytical SEC was performed to quantify the relative amount of soluble (monomeric and protofibrillar) Aβ in solution at selected time points during the aggregation experiments. For this purpose a SEC column Superdex 75 PC 3.2/30 (GE Healthcare) was connected to a Waters Separation Module 2795 equipped with a photo diode array detector (Waters Corp.). Aliquots (150 μl) of the samples were centrifuged (8500 × *g* at 4 °C for 10 min), and 50 μl of supernatant was injected into the column. Samples were individually analyzed by UV absorbance (wavelengths 210, 254, and 280 nm) at a flow rate of 0.05 ml/min.

Cell Culture Toxicity Studies

Primary Cell Cultures—Rat embryonic (E16) cortical cultures were established using a previously described procedure (44). Briefly, neurons were plated at a density of 30,000 cells/well in 96-well dishes (Costar™, Corning) previously coated with poly-L-lysine (Mr 30′000–70′000). On *in vitro* day 4, half of the medium was replaced with freshly prepared Neurobasal™ medium supplemented with 2% B27 (Invitrogen), 1× penicillin-streptomycin (Invitrogen), 0.5 mM L-glutamine, and 15 mM KCl. Subsequently, half of the medium was changed weekly. On *in vitro* day 23, half of the primary culture medium was replaced with complete Neurobasal medium containing one-fifth or one-tenth volume of amyloid peptide species with varying concentrations of $Aβ40_M$, $Aβ42_M$, $Aβ42_{PF}$, and $Aβ42_F$ and 1:1 molar mixtures thereof. Cells were subsequently incubated with Aβ species for 7 days. All amyloid peptide species were delivered in 140 mM NaCl, 10 mM Tris, pH 7.4.

Immunostaining—Cell cultures were washed with PBS and fixed with 4% paraformaldehyde (Fluka) for 15 min at 4 °C. Cultures were subsequently washed with PBS and then incubated for 1 h in a blocking solution of PBS supplemented with 10% normal goat serum (DakoCytomation) and 0.1% Triton X-100 in PBS. The cells were then incubated overnight at 4 °C in blocking solution containing mouse monoclonal anti-NeuN antibody (1/400, Chemicon Inc.). The next day, cells were washed and incubated for 2 h with a fluorescent secondary antibody (Cy3-conjugated goat anti-mouse; 1:1,000; Jackson ImmunoResearch Laboratories) followed by PBS washes. Immunostained cells were then analyzed with a BD Pathway 855 Bioimager (BD Biosciences). Images for quantitative analyses were acquired under nonsaturating exposure conditions, and image analysis was performed with NIH ImageJ software.

RESULTS

Isolation and Characterization of Protofibrillar and Monomeric Aβ—TEM images of protofibrillar Aβ42 ($Aβ42_{PF}$) fractions revealed predominantly curvilinear structures with an average length and diameter of 60–100 and 4–6 nm, respectively (supplemental Fig. 1*B*). In addition, spherical aggregates of different diameters (6–10 nm) were also observed occasionally. The second elution peak corresponding to monomeric Aβ42 ($Aβ42_M$) did not show the presence of any recognizable aggregates by TEM (supplemental Fig. 1*D*). 10–20 μM concentrations of protofibrillar and monomeric Aβ42 species converted readily into fibrils upon incubation at 37 °C (supplemental Fig. 1, *C* and *E*). After 96 h of incubation, almost all $Aβ42_M$ had aggregated into a network of long intertwining fibrils (supplemental Fig. 1*E*), whereas significant amounts of Aβ42 protofibrils persisted and coexisted with fibrils under identical conditions (supplemental Fig. 1*C*). Unlike Aβ42, Aβ40 and Aβ40-1 (reverse) eluted predominantly as a single monomeric peak under the same solubilization conditions (data not shown) and did not form fibrils under the conditions used for Aβ42 fibrillogenesis studies (supplemental Fig. 2, *A*, *C*, and *E*). Fibril formation by monomeric Aβ40 ($Aβ40_M$) required gentle agitation (300 rpm) and higher concentrations (supplemental Fig. 2, *B*, *D*, and *F*).

Monomeric Aβ40 Inhibits the Fibrillogenesis of Monomeric Aβ42 in a Concentration-dependent Manner—To probe the effects of monomeric Aβ40 interactions on the self-assembly and fibril formation of monomeric Aβ42, we co-incubated SEC-isolated $Aβ42_M$ with increasing concentrations of $Aβ40_M$ (see "Experimental Procedures"). We found that $Aβ40_M$ inhibited the fibrillogenesis of $Aβ42_M$ in a concentration-dependent manner. After co-incubation for 96 h, strong (>50%) inhibition of monomeric $Aβ42_M$ fibrillogenesis was observed in samples containing both peptides at $Aβ40_M$/$Aβ42_M$ ratios ≈ 0.5–1 (Fig. 1*A*). However, the presence of $Aβ40_M$, even at lower concentrations ($Aβ40_M$:$Aβ42_M$ ~ 0.1) led to a transient population of

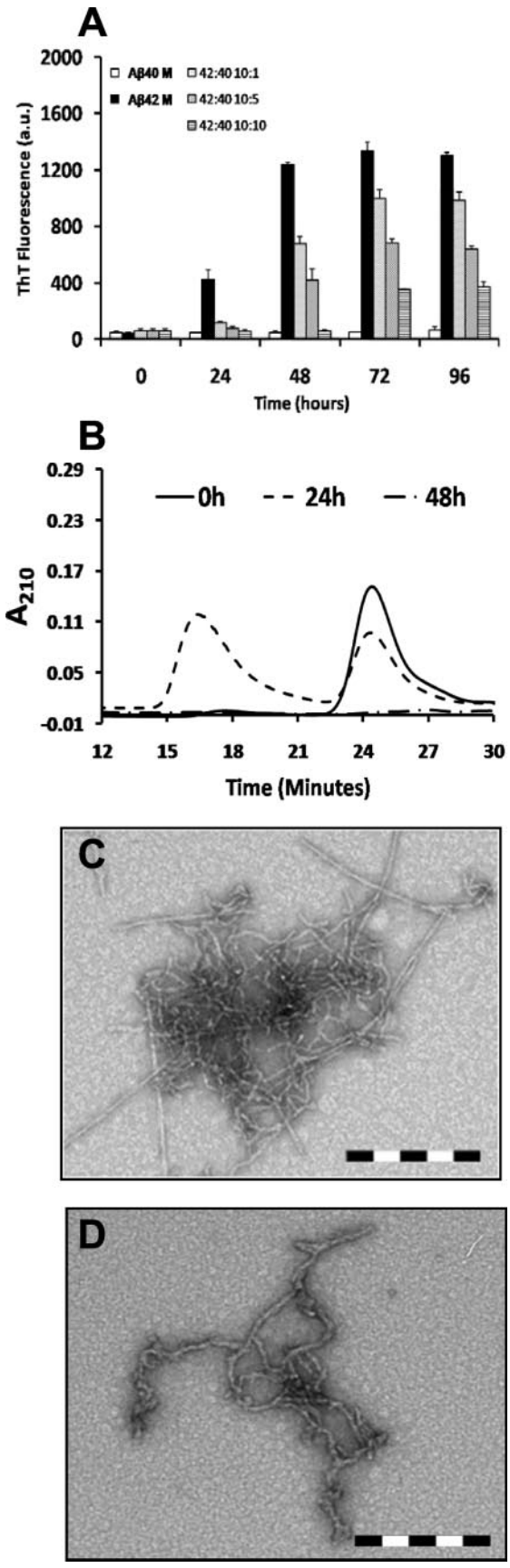

FIGURE 1. **Monomeric Aβ40 inhibits fibril formation by monomeric Aβ42 in a ratio-dependent manner and affects the structure of amyloid aggregates.** *A*, co-incubation of monomeric Aβ42 with increasing molar ratios (Aβ42$_M$:Aβ40$_M$, 10:1, 10:5, and 10:10; all final concentrations in μM) of monomeric Aβ40 results in reduced ThT binding as an inverse function of monomeric Aβ40 concentration. The *error bars* represent mean ± S.D. in duplicate samples. *M*, monomeric Aβ; *a.u.*, arbitrary units. *B*, SEC analysis on a Superdex 75 PC 3.2/30 column showing that soluble Aβ is transiently detected around 24 h of co-incubation and disappears subsequently, suggesting the formation of high molecular weight aggregates. Interestingly, co-incubation of monomeric Aβ42 with monomeric Aβ40 results in formation of various aggregate morphologies including short filamentous and protofibrillar structures. *C* and *D*, TEM images are shown for 10 μM monomeric Aβ42 incubated at 37 °C with 1 μM (*C*) and 10 μM monomer Aβ40 (*D*). *Scale bar* = 200 nm.

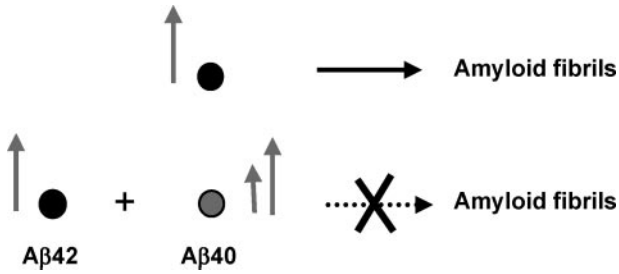

SCHEME 1. **Monomeric Aβ40 inhibits the ability of Aβ42 to form mature amyloid fibrils.** The *arrows* represent the relative concentration of each species.

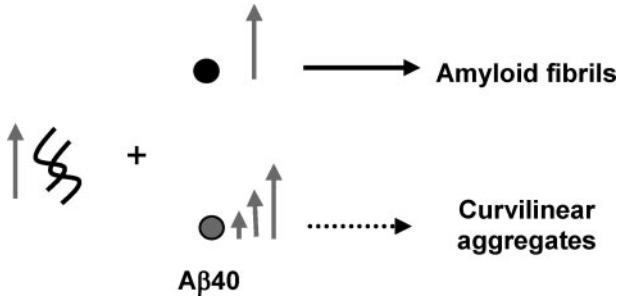

SCHEME 2. **Monomeric Aβ40 inhibits the conversion of Aβ42 into mature amyloid fibrils and favors the formation of curvilinear prefibrillar aggregates.** The *arrows* represent the relative concentration of each species.

protofibrillar species (Fig. 1*B*), which disappeared subsequently. In the absence of Aβ40, Aβ42$_M$ aggregated rapidly and formed long intertwining fibrillar networks without the accumulation of protofibrils (supplemental Fig. 1*E*). In contrast, co-incubation with Aβ40$_M$ favored the formation of short, flexible protofibrillar structures (Fig. 1, *C* and *D*, and Scheme 1), which did not appear to convert to mature elongated fibrils. Our data suggest that Aβ40$_M$ interferes with the ability of Aβ42$_M$ to form mature fibrils but does not interfere with its ability to form higher order prefibrillar aggregates. Under no conditions did we observe that mixtures of monomeric Aβ40 and Aβ42 remained as stable monomers or formed stable heterodimers on the time scale of our experiments (24–96 h).

Kinetic Stabilization of Aβ42 Protofibrils by Monomeric Aβ40—Next, we probed the interactions of monomeric Aβ (Aβ40 and Aβ42) with protofibrillar Aβ42 and assessed the consequences of such interactions on the elongation Aβ42 protofibrils into mature fibrils. For this purpose, we co-incubated Aβ42$_{PF}$ with monomeric Aβ (Aβ40$_M$ or Aβ42$_M$) at different molar ratios (Aβ$_{PF}$:Aβ$_M$, 10:1, 10:5, and 10:10; all final concentrations in μM) (Scheme 2). The addition of Aβ42$_M$ to Aβ42$_{PF}$ at increasing molar ratios resulted in enhanced ThT binding (Fig. 2*A*), consistent with the accelerated conversion of Aβ42$_{PF}$

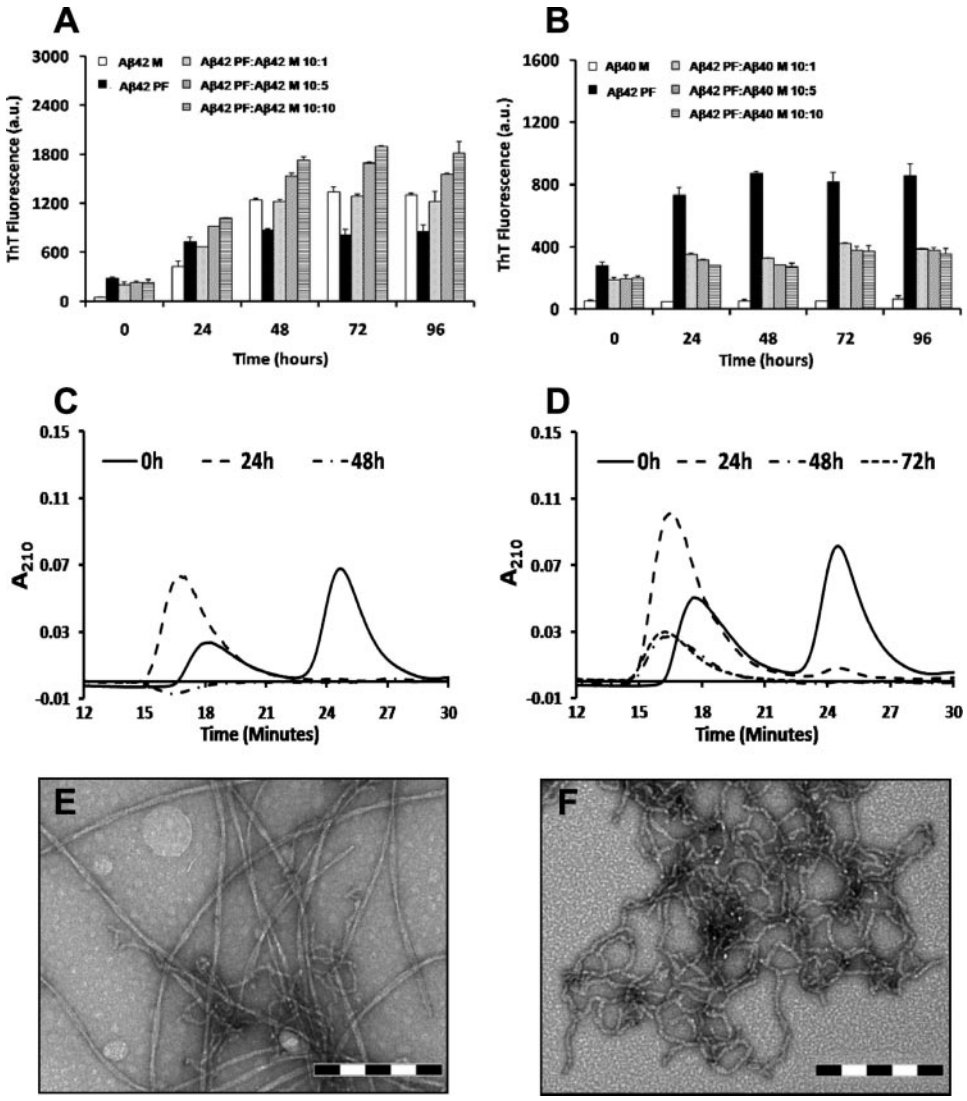

FIGURE 2. **Monomeric Aβ40 imparts kinetic stability to protofibrillar Aβ42 and retards protofibril to fibril conversion.** The addition of monomeric Aβ42 to Aβ42 protofibrils accelerates fibril formation (*A*), whereas monomeric Aβ40 disfavors fibril formation by protofibrillar Aβ42 at identical molar ratios (*B*) ($A\beta42_{PF}$:$A\beta40_{M}$, 10:1, 10:5, and 10:10; all final concentrations in μM). SEC analysis on a Superdex 75 PC 3.2/30 column revealed that addition of monomeric Aβ42 to Aβ42 protofibrils results in diminished solubility (*C*) and formation of extensive fibrillar networks (*E*). In contrast, monomeric Aβ40 promotes solubility of protofibrils over the time of co-incubation (*D*) and retards conversion of protofibrils into elongated fibrils (*F*). *Scale bar* = 200 nm. The *error bars* in *A* and *B* represent the mean ± S.D. in duplicate samples. *M*, monomeric Aβ; *PF*, protofibrillar Aβ42; *a.u.*, arbitrary units.

into mature fibrillar structures (Fig. 2*E*). SEC analysis after 48 h of co-incubation revealed that the majority of monomeric and protofibrillar Aβ42 were converted into insoluble aggregates and were no longer detectable in solution supernatant after centrifugation (Fig. 2*C*). Interestingly, the effect of $A\beta40_{M}$ co-incubation on inhibition of $A\beta42_{PF}$ fibrillar conversion was independent of ratio. In the presence of $A\beta40_{M}$, ThT fluorescence of $A\beta42_{PF}$ remained virtually unchanged even after co-incubation for 96 h (Fig. 2*B*). To determine whether the lack of a rise in ThT fluorescence was due to stabilization of $A\beta42_{PF}$ or formation of low ThT-binding Aβ aggregates, samples containing mixtures of $A\beta42_{PF}$ and $A\beta40_{M}$ were subjected to further analyses by SEC and TEM. When purified $A\beta42_{PF}$ were reinjected into an analytical Superdex 75 PC 3.2/30 SEC column, we consistently observed two peaks corresponding to $A\beta42_{PF}$ and $A\beta42_{M}$. This may have happened because $A\beta42_{PF}$ are in rapid equilibrium with monomers and/or a population of the $A\beta42_{PF}$ is more susceptible to dissociation upon interaction with the column matrix. After 24 h of co-incubation in the presence of ≥1 μM $A\beta40_{M}$, we observed a disappearance of the monomeric peak (Fig. 2*D*, 25 min), whereas the intensity and area of the protofibril peak increased (Fig. 2*D*, 18 min). Upon further incubation, the intensity and area of the protofibril peak was markedly reduced and exhibited a slight shift to higher molecular weight elution (16 min). These results suggest that the presence of $A\beta40_{M}$ blocks the formation of mature Aβ42 fibrils but does not interfere with the growth of Aβ42 protofibrils and/or possibly leads to the formation of mixed Aβ40/Aβ42 protofibrillar aggregates. This hypothesis was confirmed by TEM studies that revealed protofibrillar clusters with a predominantly curvilinear morphology for all samples containing mixtures of $A\beta42_{PF}$ and $A\beta40_{M}$ regardless of the peptide ratios (Fig. 2*F*). The average length of these aggregates was variable and significantly larger than that of SEC-isolated $A\beta42_{PF}$ (supplemental Fig. 1*B*). Of particular note, mature fibril structures similar to those formed by Aβ42 alone (Fig. 2*E* and supplemental Fig. 1*E*) were scarcely observed in samples containing mixtures of $A\beta42_{PF}$ and $A\beta40_{M}$.

Lack of Effect of Aβ40-1 on Monomeric or Protofibrillar Aβ42 Fibrillogenesis—To validate the specificity of the inhibitory effect of Aβ40 on the fibrillogenesis of monomeric and protofibrillar Aβ42, we co-incubated $A\beta42_{PF}$ or $A\beta42_{M}$ with Aβ40-1 at varying molar ratios (Aβ42:Aβ40-1, 10:1, 10:5, and 10:10; all final concentrations in μM). The results of these studies show that Aβ40-1 does not inhibit fibril formation by protofibrillar Aβ42 at any of the concentrations tested (supplemental Fig. 3*A*). However, Aβ40-1 had a small inhibitory effect on $A\beta42_{M}$ fibrillogenesis at a 1:1 ratio (supplemental Fig. 3*B*), but this activity was much less pronounced than the inhibitory affect of $A\beta40_{M}$ (Fig. 1*A*). These results underscore the specificity of the interactions between the two endogenous Aβ variants (Aβ40 and Aβ42) during amyloid fibril formation.

Monomeric Aβ40 Interferes with Growth and Reassembly of Preformed Aβ42 Fibrils—Whereas the above findings indicate that Aβ40 inhibits *de novo* fibrillogenesis of monomeric and protofibrillar Aβ42, we next sought to explore the possible

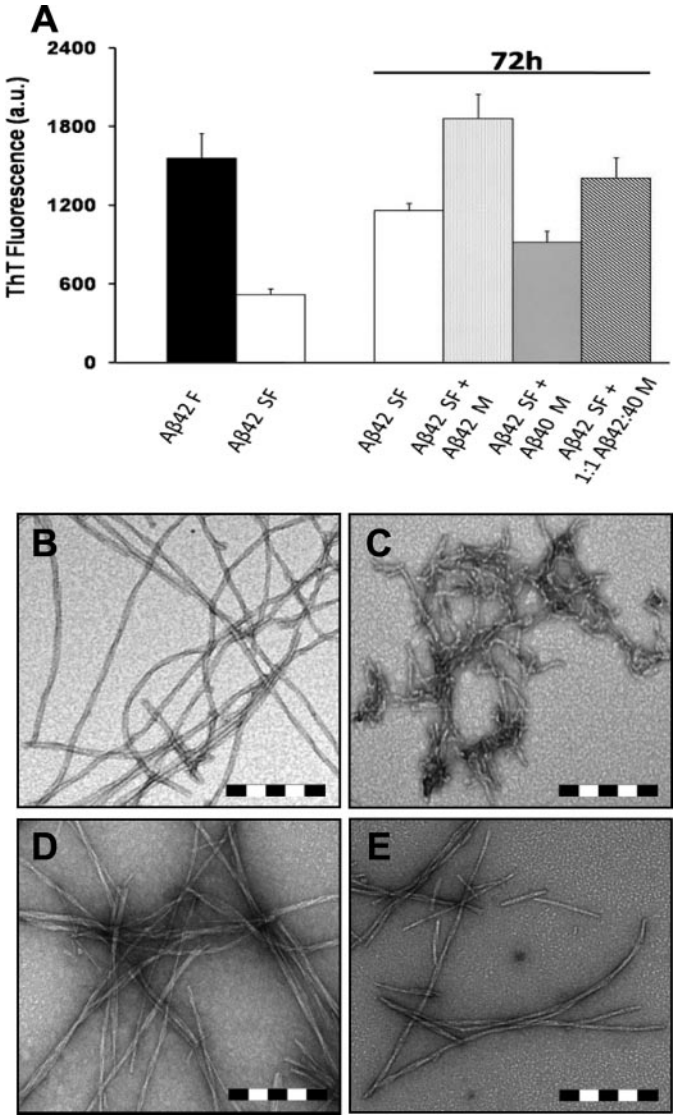

FIGURE 3. **Monomeric Aβ40 interferes with Aβ42 fibril reorganization and elongation at an equivalent ratio.** Fibrillar Aβ42 (*B*) was sonicated to generate fragmented fibrils (*C*), which were incubated at 37 °C for 72 h (*A*) in isolation (*white bar*), with 10 μM monomeric Aβ42 (*light gray dotted bar*), with 10 μM monomeric Aβ40 (*dark gray dotted bar*), and with a 1:1 mixture of the latter two (*oblique striped bar*). The addition of monomeric Aβ42 results in the resumption of fibril elongation (*D*), whereas the addition of monomeric Aβ40 at a 1:1 molar ratio to sonicated Aβ42 fibrils delays Aβ42 fibril elongation and maturation (*E*). *Scale bar* = 200 nm. The *error bars* in *A* represent the mean ± S.D. in duplicate samples. *M*, monomeric Aβ; *F*, fibrillar Aβ42; *SF*, sonicated Aβ42 fibrils; *a.u.*, arbitrary units.

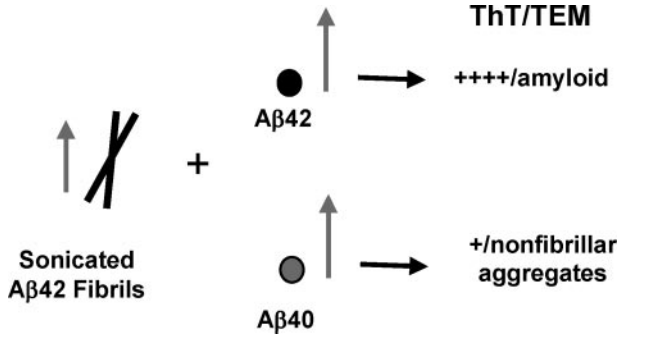

SCHEME 3. **Monomeric Aβ40 interferes with growth and reassembly of preformed Aβ42 fibrils.** The *arrows* represent the relative concentration of each species.

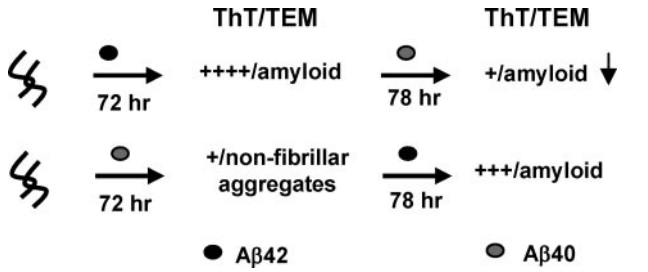

SCHEME 4. **Monomeric Aβ42 and Aβ40 compete for binding to the ends of protofibrillar and fibrillar Aβ.**

effect of Aβ40 on the growth and assembly of preexisting Aβ42 fibrils. Aβ42 fibrils were mechanically disrupted by ultra-sonication to generate a narrow distribution of small, 100–300-nm-long fibrillar structures with an average diameter of 10 to 12 nm (Fig. 3, *B* and *C*). The sonicated Aβ42 fibrils ($Aβ42_{SF}$) were allowed to reassociate at 37 °C as follows: (i) in isolation; (ii) in the presence of $Aβ42_M$ (10 μM); (iii) in the presence of $Aβ40_M$ (10 μM); or (iv) in the presence of a 1:1 mixture of $Aβ42_M$ and $Aβ40_M$ (20 μM final Aβ concentration) (Scheme 3). Upon incubation for 72 h at 37 °C, the fragmented Aβ42 fibrils reassociated to form elongated fibrils with morphological features similar to the parent fibrils (data not shown). The addition of $Aβ42_M$ to fragmented fibrils accelerated fibril growth and led to the emergence of mature fibrillar structures (Fig. 3, *A* and *D*), whereas the addition of $Aβ40_M$ retarded their growth and blocked fibril reassembly as evidenced by significantly reduced ThT fluorescence (Fig. 3*A*). TEM images of the fragmented fibrils incubated in the presence of $Aβ40_M$ also revealed predominantly truncated fibrillar aggregates and the absence of mature fibrils (Fig. 3*E*). Co-incubation of sonicated Aβ42 fibrils with a 1:1 mixture of $Aβ42_M$:$Aβ40_M$ resulted in fibril growth and reassembly but to a lesser extent than seen after $Aβ42_M$ addition (data not shown). These observations suggest that Aβ40, at near equimolar ratios, retards the elongation and maturation of fragmented Aβ42 fibrils into classical ThT-binding amyloid fibrils (as shown in Figs. 2*E* and 3*B* and supplemental Fig. 1*E*).

Monomeric Aβ42 and Aβ40 Are Constantly Recycled and Compete for Binding to the Ends of Protofibrillar and Fibrillar Aβ Aggregates—The above observations highlight a significant degree of molecular cross-talk between Aβ40 and different aggregation states of Aβ42 (monomer, protofibrils, and fibrils) during amyloid fibril formation. Hence, we ventured to further explore this phenomenon and probe the dynamics of exchange between monomeric Aβ42 and Aβ40 at the end of protofibrillar and fibrillar forms of Aβ42. For this purpose, Aβ42 protofibrils (10 μM) were incubated in presence of $Aβ42_M$ (10 μM), $Aβ40_M$ (10 μM), or a 1:1 mixture of both peptides (20 μM final Aβ concentration) for 72 h (Fig. 9). After this, a second 10 μM addition of freshly prepared monomeric Aβ species ($Aβ42_M$, $Aβ40_M$, or $Aβ42_M$ plus $Aβ40_M$) was carried out, and the resultant mixtures were incubated for an additional 78 h (150 h total) (Scheme 4). At each step of the process, the presence of fibrils was monitored by ThT binding and negative staining TEM. As expected, the addition of $Aβ42_M$ to $Aβ42_{PF}$ resulted in enhanced ThT fluorescence (Fig. 4*A*, *II*, 72 h) and the formation

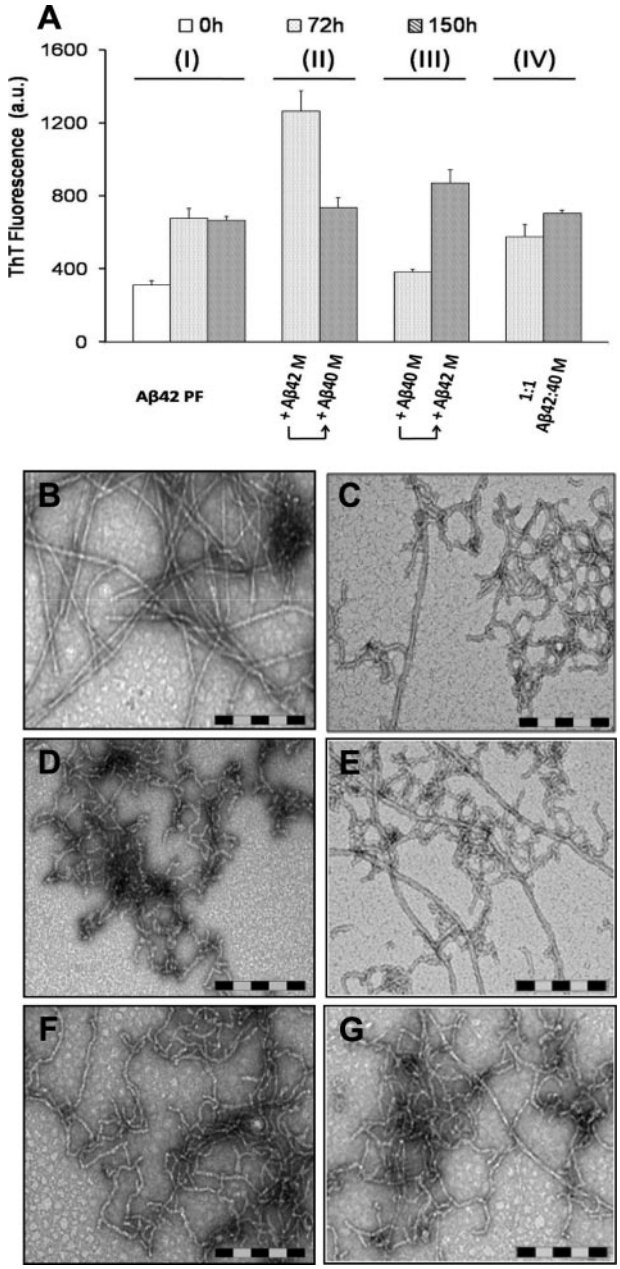

FIGURE 4. **Monomeric Aβ40 and Aβ42 exchange along different stages of amyloid formation imparts distinct structural features on amyloid aggregates.** Aβ42 protofibrils were exposed to sequential addition of either monomeric Aβ42 or monomeric Aβ40 for an extended period of time (*A*) (see "Experimental Procedures" and Fig. 8 for details). When added to Aβ42 fibrils, monomeric Aβ40 alters the fibrillar structure (*B*) and leads to the emergence of curvilinear morphologies (*C*). Moreover, the addition of monomeric Aβ42 to Aβ40-stabilized protofibrils (*D*) results in conversion of protofibrillar structures into elongated fibrils (*E*). When added to Aβ42 protofibrils, a 1:1 mixture of monomeric Aβ42 and Aβ40, delays the emergence of mature fibrils (72 h (*F*) and 150 h (*G*)). *Scale bar* = 200 nm. The *error bars* in *A* represent the mean ± S.D. in duplicate samples. *M*, monomeric Aβ; *PF*, protofibrillar Aβ42; *a.u.*, arbitrary units.

of dense fibrillar networks (Fig. 4*B*). Interestingly, when $A\beta40_M$ was added to this fibrillized Aβ42 and incubated for an additional 78 h, ThT fluorescence was substantially reduced (Fig. 4*A*, *II*, 150 h), and in addition to fibrils, a substantial amount of curvilinear, non-fibrillar structures were also observed (Fig. 4*C*). In contrast, when $A\beta42_{PF}$ were co-incubated with $A\beta40_M$ for 72 h, there was a negligible rise in ThT fluorescence (Fig. 4*A*, *III*, 72 h), and non-fibrillar structures resembling protofibrils were observed as the predominant species (Fig. 4*D*). However, the addition of $A\beta42_M$ overcame the stabilizing effect of Aβ40 on protofibrils, resulted in enhanced ThT fluorescence (Fig. 4*A*, *III*, 150 h), and led to emergence of long mature fibrils (Fig. 4*E*). Finally, serial additions of a 1:1 mixture of monomeric $A\beta42_M$: $A\beta40_M$ to Aβ42 protofibrils resulted in a slight rise in ThT fluorescence relative to that obtained upon the addition of $A\beta40_M$ alone (Fig. 4*A*, *IV*). An examination of this sample by TEM revealed mainly curvilinear non-fibrillar structures and short protofibrils (Fig. 4, *F* and *G*). The observation that $A\beta40_M$ can alter the structure of preformed $A\beta42_F$ supports the notion that Aβ40 and Aβ42 monomers are exchangeable at the growing ends of amyloid aggregates (protofibrils and fibrils).

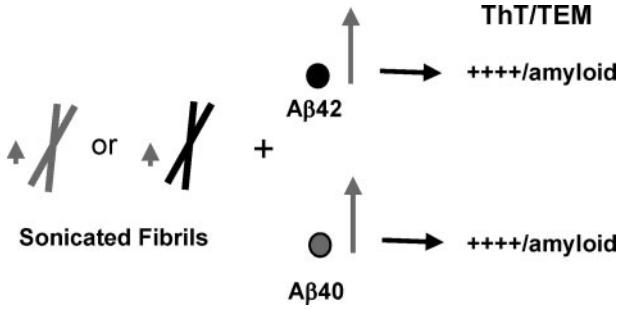

SCHEME 5. **Aβ42 fibrils nucleate the fibrillogenesis of monomeric Aβ40 and vice versa.**

Seeding Polymerization of Monomeric Aβ (Aβ42 and Aβ40) with Protofibrillar and Fibrillar Aβ (Aβ42 and Aβ40)—Amyloid fibril formation occurs via a nucleation-dependent polymerization process akin to protein crystallization (45, 46). Conventionally, a nucleated polymerization process is divisible into three closely related phases: (i) a slow nucleation "lag" phase comprising thermodynamically unfavorable interactions of protein molecules leading to the formation of nuclei (or seeds); (ii) an elongation phase leading to the emergence of higher order aggregates (fibrils); and lastly, (iii) a steady-state phase in which there is a dynamic equilibrium between the fibrils and monomers in solution (46). The duration of lag phase is significantly shortened in the presence of preformed "nuclei" or "seeds," which promote accelerated self-assembly and amyloid formation by monomeric protein (47). This seeding effect has also been demonstrated to be a sequence-specific process (48–50).

Aβ42 Fibrils Nucleate the Fibrillogenesis of Monomeric Aβ40 and Vice Versa—Previous studies have established the ability of Aβ fibrils to induce fibril formation by monomeric Aβ through the process of nucleated polymerization (22, 38). Thus, we sought to explore the ability of both well characterized protofibrillar and fibrillar forms of Aβ42 to seed the fibrillogenesis of monomeric Aβ40 and Aβ42. For these experiments, we isolated aggregate-free monomeric Aβ40 and Aβ42 by SEC and characterized its fibrillogenesis in the presence of different amounts of fibrillar seeds of either Aβ40 or Aβ42 (sonicated fibrils of $A\beta42_{SF}$ at 10 and 20 μg/ml and sonicated fibrils of $A\beta40_{SF}$ at 10 and 20 μg/ml) (Scheme 5). $A\beta42_M$ (20 μM) alone (with no seeds) exhibited an appreciable rise in ThT binding after 15 h and reached a plateau after 50 h of incubation at 37 °C. The addition of sonicated fibrils of $A\beta42_{SF}$ abolished the lag

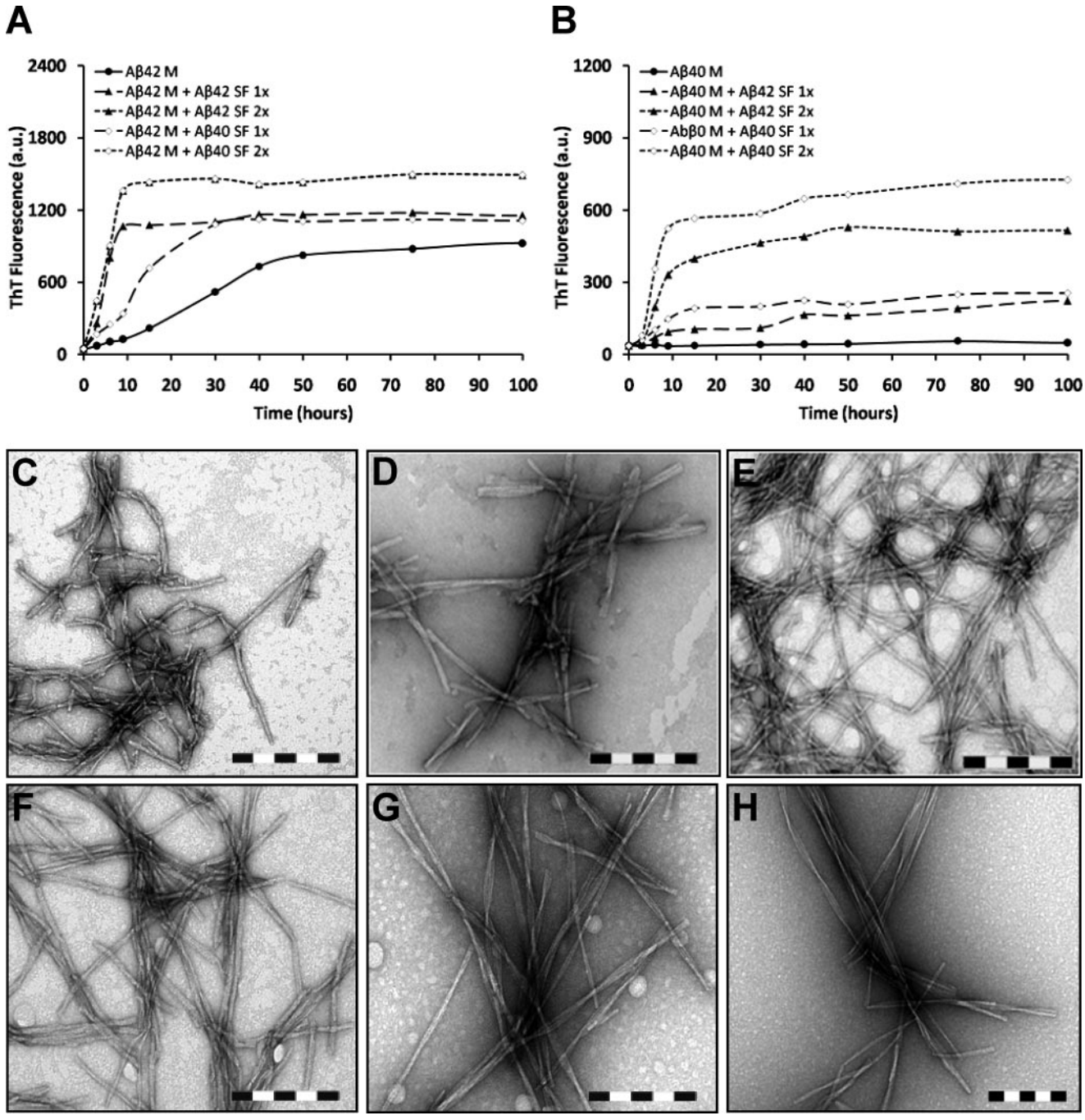

FIGURE 5. **Aβ (Aβ40 and Aβ42) fibrils induce polymerization of monomeric Aβ (Aβ40 and Aβ42), and the structure of resultant amyloid fibrils is determined by monomeric Aβ.** Fibril formation by 20 μM monomeric Aβ ($A\beta40_M$ and $A\beta42_M$) was induced by two different concentrations (10 and 20 μg/ml) of fibrillar Aβ42 (*C*) or fibrillar Aβ40 (*D*). The addition of fibrillar Aβ (Aβ40 or Aβ42) to monomeric Aβ42 abolishes the lag phase of fibril formation, and similar equilibrium levels are achieved regardless of the nature and concentration of fibrillar seeds added (*A*). In contrast, when monomeric Aβ40 aggregation is seeded with fibrillar Aβ (Aβ40 or Aβ42), although the lag phase is shortened, steady-state levels depend on the amount of fibrillar seeds added (*B*). Electron microscopic images of monomeric Aβ42 aggregation seeded with fibrillar Aβ42 (*E*) and fibrillar Aβ40 (*F*), along with monomeric Aβ40 aggregation seeded with fibrillar Aβ42 (*G*) and fibrillar Aβ40 (*H*), reveal that the structure of the resultant amyloid fibrils is determined by the monomeric Aβ regardless of the nature and concentration of fibrillar Aβ added as seeding effectors. *Scale bar* = 200 nm. ThT data were normalized by subtracting the ThT fluorescence values obtained from incubation of sonicated fibrils (10 and 20 μg/ml) in isolation. *M*, monomeric Aβ; *SF*, sonicated Aβ fibrils; 1× = 10 μg/ml; 2× = 20 μg/ml; *a.u.*, arbitrary units.

phase and reduced the time required to reach near equilibrium levels of fibril formation (~9–15 h) (Fig. 5*A*). Interestingly, addition of sonicated fibrils of $A\beta40_{SF}$ also decreased lag phase time but exhibited a longer time to reach near equilibrium (~25–30 h) (Fig. 5*A*). Regardless of the seeding species, $A\beta42_M$ forms similar fibrils that are ≥1 μm long and have diameters of 10–14 nm. These fibrils appear to be composed of 2–3 protofilaments and exhibit a helical twist spaced at 60–180 nm (Fig. 5, *E* and *F*). For the purpose of discussion, we will refer to these fibrils as type I Aβ fibrils.

In parallel, we investigated the ability of $A\beta40_{SF}$ and $A\beta42_{SF}$ to seed the fibrillogenesis of monomeric Aβ40. For this purpose, $A\beta40_M$ (20 μM) was co-incubated with $A\beta42_{SF}$ (10 and 20 μg/ml) and $A\beta40_{SF}$ (10 and 20 μg/ml). It is noteworthy that

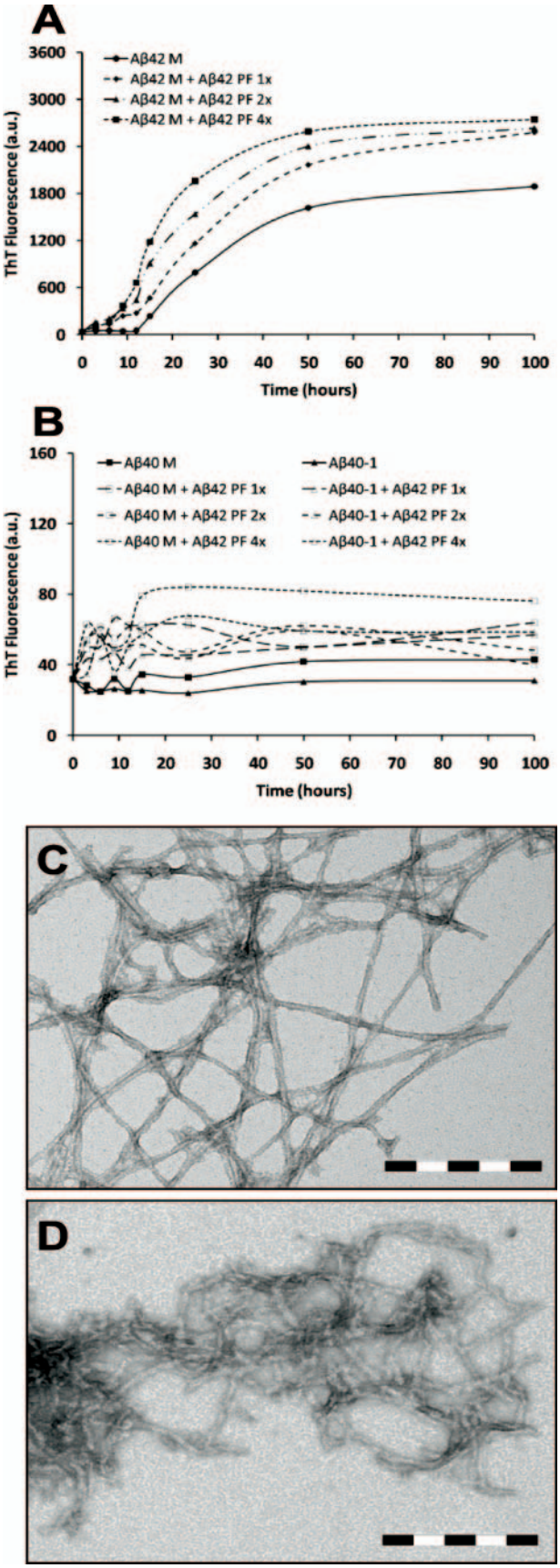

FIGURE 6. **Aβ42 protofibrils do not serve as efficient seeding nuclei for Aβ40 fibril formation.** Fibril formation by 20 μM monomeric Aβ (Aβ40 and Aβ42) was induced at three different concentrations (1, 2, and 4 μM) of protofibrillar Aβ42. The addition of protofibrillar Aβ42 to monomeric Aβ42 abolishes the lag phase of fibril formation in a concentration-dependent fashion (*A*) and promotes fibril formation (*C*). In contrast, no seeding effect is observed when similar concentrations of protofibrillar Aβ42 are added to the solution containing monomeric Aβ40 (*B*), and predominantly curvilinear structures, reminiscent of protofibrils, are observed (*D*). *Scale bar* = 200 nm. ThT data were normalized by subtracting the ThT fluorescence values obtained from incubation of Aβ42 protofibrils (1, 2, and 4 μM) in isolation. *M*, monomeric Aβ; *PF*, protofibrillar Aβ42; 1× = 1 μM; 2× = 2 μM; 4× = 4 μM; *a.u.*, arbitrary units.

$A\beta40_M$ (20 μM) alone (with no seeds), under stagnant conditions, did not form amyloid fibrils during the time scale of these experiments (Fig. 5*B* and supplemental Fig. 2, *A* and *E*) but formed fibrils readily at higher concentrations or under agitating conditions (supplemental Fig. 2, *B* and *F*). When $A\beta40_{SF}$ or $A\beta42_{SF}$ was added to the solution of monomeric Aβ40, we observed two distinct effects on Aβ40 assembly: (i) the elongation phase was sensitive to the concentration of seeding fibrils, and (ii) at all time points, the level of ThT binding near equilibrium was relatively higher in the presence of $A\beta40_{SF}$ than of $A\beta42_{SF}$, suggesting preferential seeding in the presence of $A\beta40_{SF}$ (Fig. 5*B*). Moreover, $A\beta40_M$ generated similar fibrils regardless of the nature and amount of seeding species (Fig. 5, *G* and *H*). The resulting fibrils had variable lengths with diameters of 6 to 14 nm. The fibrils formed by of Aβ40 consisted of ≥3 protofilaments and exhibited a helical periodicity of 110 to 180 nm. TEM analysis of a 20 μM $A\beta40_M$ sample incubated under identical conditions for 100 h did not show any fibrils (data not shown).

Aβ42 Protofibrils Seed the Fibrillogenesis of Monomeric Aβ42 but Not Monomeric Aβ40—To explore the ability of Aβ42 protofibrils to seed the fibrillogenesis of monomeric Aβ (Aβ40 and Aβ42), we co-incubated 20 μM monomeric Aβ ($A\beta40_M$ or $A\beta42_M$) with three different molar ratios of $A\beta42_{PF}$ (*i.e.* $A\beta_M$:$A\beta42_{PF}$ at 20:1, 20:2, and 20:4; all final concentrations in μM). We found that even the lowest concentration of $A\beta42_{PF}$ (1 μM) was sufficient to accelerate the fibrillogenesis of monomeric Aβ42 (Fig. 6*A*), whereas no such effect was observed (for any molar ratio) when $A\beta42_{PF}$ were added to monomeric Aβ40 under identical conditions (Fig. 6*B*). TEM analysis of these co-incubation samples confirmed the validity of the above mentioned observations such that when protofibrillar Aβ42 was added to monomeric Aβ42, extended networks of fibrillar structures were observed at all molar ratios ($A\beta42_M$:$A\beta42_{PF}$, 20:4 μM (Fig. 6*C*)). In contrast, the addition of $A\beta42_{PF}$ to $A\beta40_M$ resulted in the formation of mainly short flexible non-fibrillar structures ($A\beta40_M$:$A\beta42_{PF}$, 20:4 μM (Fig. 6*D*)). The absence of mature Aβ40 fibrils indicates that Aβ42 protofibrils are less efficient as seeding nuclei for Aβ40 fibrillogenesis as compared with fibrillar Aβ42.

In parallel, we co-incubated 20 μM Aβ40-1 with sonicated fibrils of Aβ ($A\beta40_{SF}$ or $A\beta42_{SF;}$ 20 μg/ml) or protofibrillar $A\beta42_{PF}$ (4 μM) as control experiments. Neither fibrillar Aβ ($A\beta40_{SF}$ and $A\beta42_{SF}$) nor protofibrillar $A\beta42_{PF}$ resulted in fibril formation from Aβ40-1 (supplemental Fig. 5).

Treatment of Cultured Neurons with Specific Aggregation-prone Aβ Species or Mixtures Is Associated with Decreased Neuronal Viability—To assess the differential effects of monomeric Aβ (Aβ40 or Aβ42) on the toxicity of Aβ42 aggregates to pri-

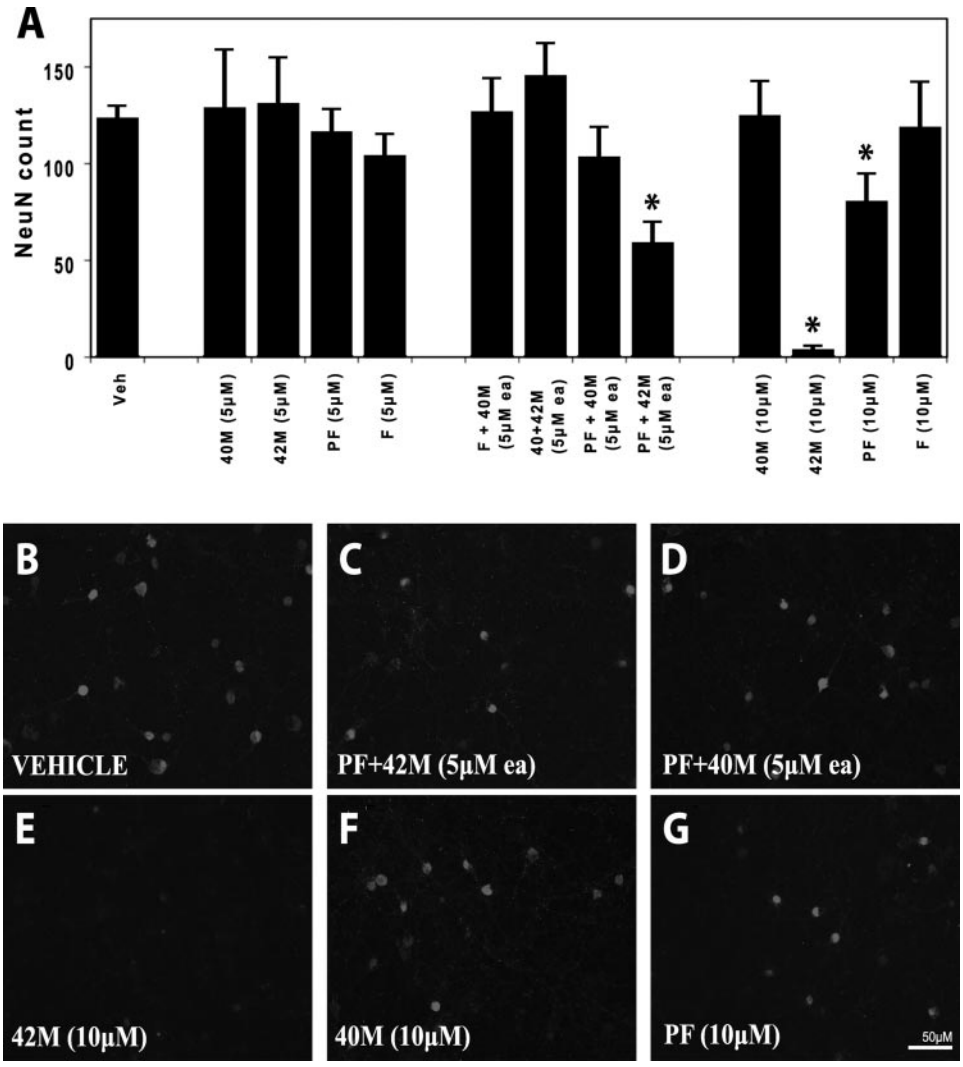

FIGURE 7. **Conditions favoring accelerated aggregation of Aβ42 *in vitro* are associated with enhanced neurotoxicity.** Cultured rat E16 primary cortical neurons were treated for 7 days with Aβ40 (monomeric), Aβ42 (monomeric, protofibrillar, and fibrillar) or 1:1 mixtures thereof, as indicated under "Experimental Procedures." Cell viability was quantified after immunostaining for the neuronal marker, neuronal nuclei (*NeuN*). Graphs represent the means ± S.E. of at least five replicates. Treatment with 10 μM Aβ42 protofibrils (*A* and *G*) caused significant (*t* test; *, $p < 0.01$), but milder toxicity than 10 μM monomeric Aβ42 (*A* and *E*) or a mixture of monomeric and protofibrillar Aβ42 (*A* and *C*) (5 μM each) (*t* test; *, $p < 0.002$). In contrast, cells exposed to 10 μM monomeric Aβ40 (*A* and *F*), 10 μM Aβ42 fibrils (*A*), or a mixture of monomeric Aβ40 and protofibrillar Aβ42 (5 μM each; *A* and *D*) did not show significant neurotoxicity. *Veh*, vehicle.

mary cortical neurons, we applied these species to cultured E16 rat cortical neurons. Cell survival was measured by the numbers of surviving NeuN-positive cells after 7 days of treatment (see "Experimental Procedures"). $Aβ40_M$ showed no significant effect on neuronal viability at concentrations between 0.1 and 10 μM (Fig. 7, *A* and *F*, and supplemental Fig. 6), consistent with its reduced propensity to aggregate and fibrillize *in vitro*. At concentrations from 0.1 to 5 μM, neither $Aβ42_M$ nor $Aβ42_{PF}$ had an effect on neuronal viability (Fig. 7*A* and supplemental Fig. 6). Interestingly, when 5 μM monomeric Aβ (Aβ40 or Aβ42) was mixed with $Aβ42_{PF}$, only the mixtures containing $Aβ42_M$ resulted in significant loss of neuron viability ($n = 5$ $p < 0.002$; Fig. 7, *A*, *C*, and *D*). To determine whether the decrease in neuronal viability was due to an increase in the total concentration of Aβ42, we probed the effect of monomeric, protofibrillar, and fibrillar forms of Aβ42 on neuronal viability at 10 μM concentration. Both monomeric and protofibrillar Aβ42, but not Aβ42 fibrils, caused significant reduction in neuronal viability, with monomeric Aβ42 consistently showing a pronounced effect ($Aβ42_M$: $n = 5$ $p < 10^{-5}$ (Fig. 7, *A* and *E*); $Aβ42_{PF}$: $n = 5$ $p < 0.01$ (Fig. 7, *A* and *G*)). Exposure to a 1:1 mixture of $Aβ42_M$ and $Aβ40_M$ (5 μM each) had no effect on neuronal viability (Fig. 7*A*). These results support a central role of Aβ42 in neurotoxicity as well as the notion that Aβ-mediated cell death requires ongoing nucleation-dependent polymerization of Aβ42 (51).

DISCUSSION

Increasing evidence from genetics, clinical, and cell culture studies suggests that the ratio of Aβ40 to Aβ42, rather than the total amount of Aβ, is an important determinant of Aβ aggregation, fibrillogenesis, and toxicity (52). However, the molecular mechanisms by which changes in this ratio alter the aggregation, clearance, and distribution of Aβ *in vivo* remain uncertain. Similar studies reported previously have examined the effects of single Aβ species or total Aβ concentrations (Aβ40 + Aβ42) but have not explored the interactions of distinct Aβ aggregate states (*e.g.* monomers, oligomers, protofibrils, and fibrils). Given that both Aβ42 and Aβ40 peptides exist in equilibrium between these different states *in vivo*, it is crucial to determine how the interactions between distinct aggregation states of each peptide influence Aβ aggregation, fibril formation, and cellular toxicity. In the present work, we have uncovered new aspects of Aβ aggregation equilibria by investigating the ratio-dependent effects of monomeric Aβ40 on the fibrillogenesis of monomeric and protofibrillar forms of Aβ42 and the dynamic reassembly of short Aβ42 fibrils. By studying well defined aggregation states of Aβ, our findings provide critical new mechanistic insights about how Aβ40 and Aβ42 interact at different stages along the amyloid formation pathway. These findings have allowed us to develop a new working model of Aβ42 and Aβ40 interactions, which could serve as mechanistic explanation for *in vivo* amyloid formation (Fig. 9).

The Ratio of Aβ42 Aggregates to Monomeric Aβ40 Is an Important Determinant of Aβ Aggregation and Fibrillogenesis—The *in vitro* studies presented here demonstrate that maintain-

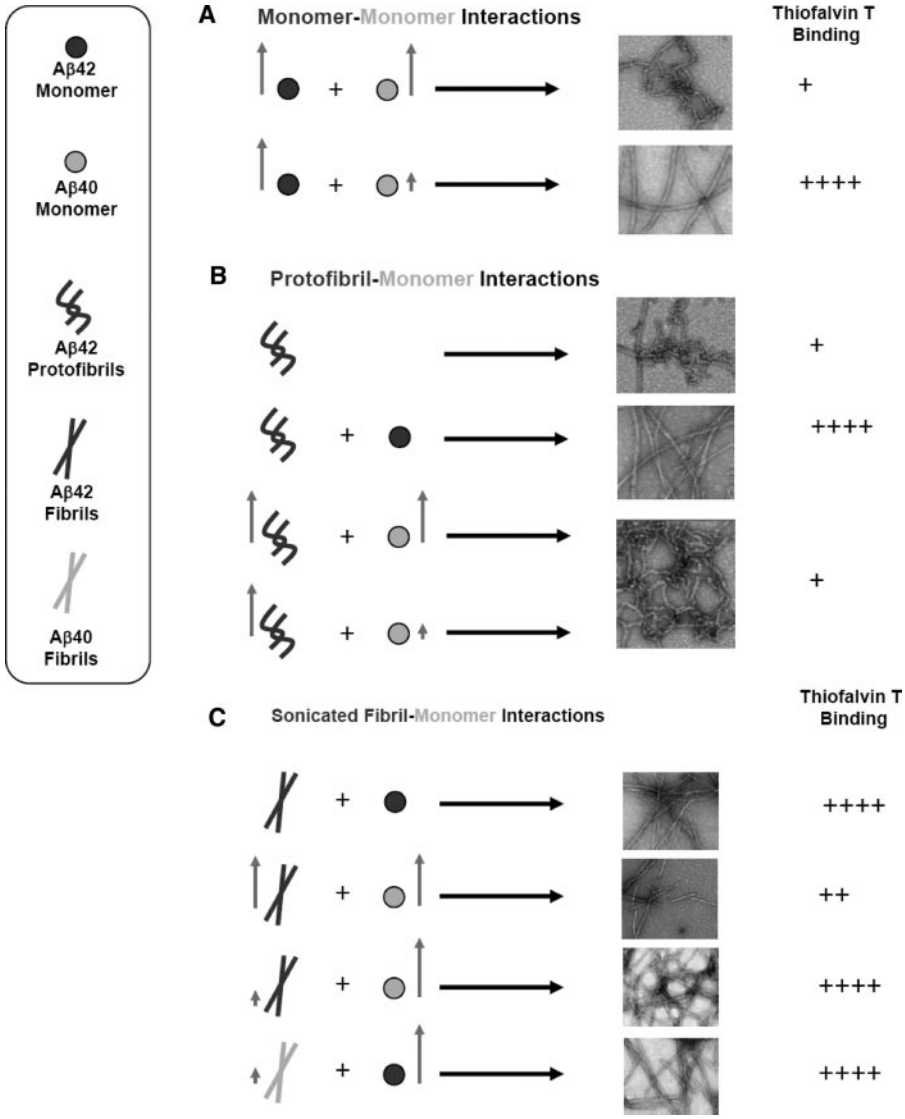

FIGURE 8. **The ratio of monomeric (Aβ40 and Aβ42) to aggregated forms of Aβ40 and Aβ42 is an important determinant of Aβ aggregation and fibrillogenesis.** This is a schematic illustration of the effect of monomeric $A\beta40_M$ on the fibrillogenesis of the monomeric (*A*), protofibrillar (*B*), and fibrillar (*C*) forms of Aβ42. Aβ40 and Aβ42 species (M, PF, and F) are depicted in *grey* and *black*, respectively. The level of ThT dye binding and fluorescence observed for the final aggregates formed in each of the experiments listed is indicated by *plus signs*: +++++ is indicative of high ThT fluorescence, and + is indicative of low ThT fluorescence.

ing a delicate balance not only between the monomeric forms of Aβ42 and Aβ40 but also between the monomeric and aggregated forms of both peptides is essential for maintaining Aβ solubility and preventing Aβ fibrillogenesis and toxicity. First, in the presence of excess $A\beta40_M$ (as is expected under normal physiological conditions), $A\beta42_M$ aggregation is discouraged because of its low concentration and the inhibitory effect of excess $A\beta40_M$. As the concentration of $A\beta42_M$ increases (due to FAD-associated mutations in APP or other local factors), the formation of high molecular weight protofibrillar aggregates or low ThT-binding fibrillar structures is favored (Fig. 8). The molecular size, kinetic stability, and potential toxicity of such species depend on the local concentration of Aβ40 at the site of their formation or localization. The stabilization of protofibrillar and/or low ThT-binding Aβ aggregates could explain the lack of clear correlation between amyloid plaque pathology and cognitive decline in patients with AD (53–55). Figs. 8 and 9 summarize the effect of the ratio of monomeric (Aβ40 and Aβ42) to aggregated forms of Aβ40 and Aβ42 in the structural and ThT binding properties of the resultant Aβ aggregates. At higher $A\beta42_M/A\beta40_M$ ratios, amyloid fibril formation is favored and can be accelerated by seeding with fibrils of either Aβ40 or Aβ42. At $A\beta40_M/A\beta42_{PF}$ and $A\beta40_M/A\beta42_F$ ratios of 0.5 to 1, the formation of mature amyloid fibrils is inhibited, and predominantly protofibrillar and/or low ThT binding fibrils are formed. Interestingly, Aβ42 fibrils seed the fibrillogenesis of both peptides (Aβ40 and Aβ42); however, Aβ42 protofibrils were found to seed the fibrillogenesis of monomeric Aβ42 but not of monomeric Aβ40. These observations support the notion that Aβ42 is more highly fibrillogenic and plays a crucial role in the initiation and progression of Aβ aggregation.

Aβ42 Fibril Growth and Reassembly Is Modulated by Constant Recycling and Competition between Monomeric Aβ40 and Aβ42—Previous studies have shown that amyloid fibril growth occurs by monomer addition to the growing fibril ends (56–59). In addition, NMR and mass spectrometry studies have also shown that monomeric subunits constantly recycle in and out of the fibrillar backbone (60, 61). Given our findings that Aβ40 inhibits the fibrillogenesis of monomeric and protofibrillar Aβ42, we hypothesized that Aβ40 also intervenes in the growth and reassembly of Aβ42 fibrils. We envisioned that his could occur by several mechanisms, two of them being; (i) by competing at the free ends of Aβ42 fibrils and preventing addition of monomeric Aβ42; or (ii) by interacting and sequestering free monomeric Aβ42 in solution and preventing its docking back into Aβ42 fibrils. To test these two possibilities, we examined the effect of Aβ40 on the growth and reassembly of fragmented Aβ42 fibrils (see "Experimental Procedures"). In the presence of excess monomeric Aβ42, the fragmented Aβ42 fibrils grew and reassembled rapidly to form fibrillar structures identical to that of the parent fibrils (Figs. 3*B* and 9). In contrast, the addition of monomeric Aβ40 retarded Aβ42 fibril reassembly, led to the accumulation of truncated fibrillar structures that exhibited low ThT binding and did not convert to mature fibrils in our experimental time scale (up to

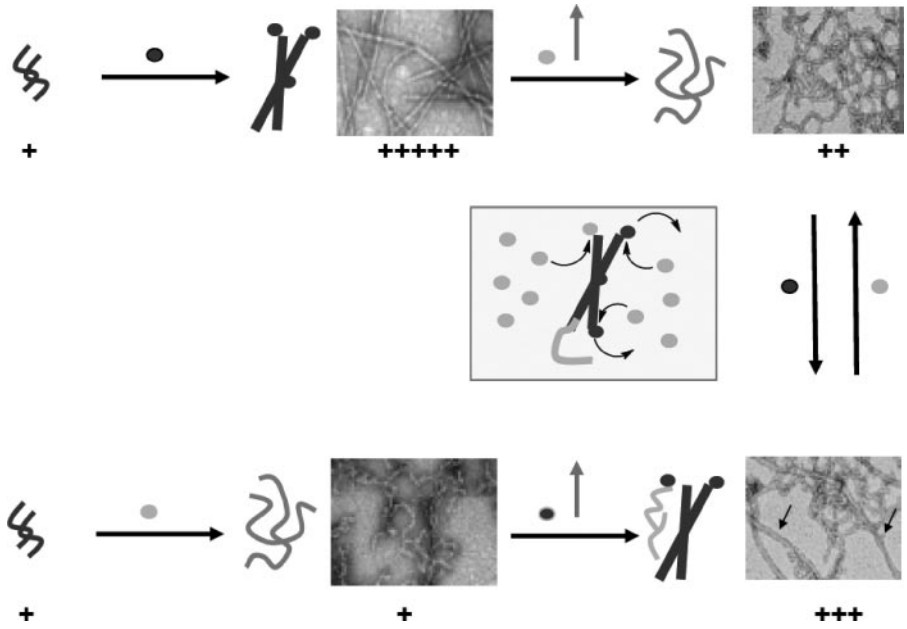

FIGURE 9. **Aβ42 fibril growth and reassembly is modulated by constant recycling and competition between monomeric Aβ40 and Aβ42.** This is a schematic depiction of the dynamic exchange between Aβ42 and Aβ42 monomers at the ends of Aβ42 aggregates and the consequences of such an exchange on the Aβ42 fibrillar morphology and ThT dye binding.

150 h). Extending this approach further, we carried out sequential additions of monomeric Aβ42 and monomeric Aβ40 to different Aβ aggregation states (Fig. 9). The addition of monomeric Aβ40 to Aβ42 protofibrils resulted in the formation of curvilinear, non-fibrillar aggregates (Figs. 4*D* and 9). However, upon reintroduction of monomeric Aβ42, these structures disappeared, and mature amyloid fibrils of Aβ42 emerged as the predominant species (Fig. 4*E*). These observations provide experimental support for the recycling and exchange of monomeric Aβ42 and monomeric Aβ40 at the growing ends of Aβ aggregates (protofibrillar and fibrillar). This is consistent with recent NMR-based reports that Aβ40, when added to the solution of aggregated Aβ42, is capable of displacing Aβ42 monomers with the latter being recycled into solution (41). Studies are currently under way to determine quantitatively the rate of monomer exchange or preferential incorporation of Aβ40 or Aβ42 monomers into Aβ42 aggregates (protofibrils and fibrils).

The fact that Aβ42 fibrils continue to grow, albeit slowly, when co-incubated with monomeric Aβ40 indicates that Aβ40 can dock and self-assemble on the free ends of Aβ42 fibrils, thus resulting in the formation of mixed fibrils (Fig. 3, *A* and *E*) (56). This latter observation also suggests that Aβ40 inhibits the formation of mature amyloid fibrils by Aβ42 but does not block self-assembly into non-fibrillar aggregates (Fig. 9). Furthermore, at $A\beta40_M/A\beta42_M$ ratios of 0.5 to 1, we observed nearly complete conversion of monomeric Aβ40 and Aβ42 into high molecular aggregates over time (Fig. 1*B*). This latter finding suggests that Aβ40-mediated inhibition of Aβ42 fibrillogenesis is due to its interaction with some oligomeric/aggregated form(s) of Aβ42 rather than to the formation of stable Aβ heterodimers.

Kinetic Stabilization of Aβ42 Aggregates by Aβ40 May Underlie Its Effect on Aβ Aggregation, Toxicity, and Pathology Distribution in Vivo—The transient formation of protofibrils during the fibrillogenesis of almost all amyloid forming proteins supports the notion that protofibrils are obligate intermediates that are likely to exist, at least transiently, *in vivo*. Aβ protofibrils and oligomers (dimers, trimers, up to dodecamers) have been prepared *in vitro* from synthetic peptides or purified from conditioned media of APP-overexpressing cells (62, 63), are biologically active entities (64), and bind, albeit weakly, to the amyloid-specific dyes such as ThT and Congo red (65). Several independent studies have implicated Aβ protofibrils as the predominant toxic species through effects that include inhibition of long term potentiation (64, 66), disruption of signal transduction (67), and formation of channels or pores in cellular membranes (68–70). These findings have led to the hypothesis that conversion of small toxic Aβ aggregates into fibrils, and their sequestration within inclusions or plaques, is neuroprotective and may represent an active natural detoxification mechanism (71). Hence, it can be argued that factors that alter the distribution and/or kinetic stability of Aβ protofibrils should influence their aggregation and toxicity *in vivo*. Therefore, stabilizing a toxic population of protofibrils should enhance toxicity and accelerate disease progression. In contrast, stabilization of a nontoxic protofibrillar or fibrillar forms of Aβ may have beneficial effects. In fact, a recent report suggests that reducing the lifetime of protofibrils by accelerating their conversion into amyloid fibrils protects against Aβ induced toxicity (72).

Our study demonstrates that Aβ40 enhances the kinetic stability of Aβ42 protofibrils and, at high concentrations, promotes the formation of low ThT-binding aggregates. This could provide possible mechanistic explanations for the effect of the ratio of Aβ40 to Aβ42 on the distribution of amyloid pathology (parenchymal *versus* vascular). In the presence of high $A\beta40_M/A\beta42_F$ or $A\beta42_M/A\beta40_F$ ratios ($\geq$10), Aβ fibril formation is accelerated and leads to local accumulation of fibrillar aggregates in brain parenchyma. In contrast, subphysiologic $A\beta40_M/A\beta42$ (monomeric or protofibrillar) ratios (0.5–2) favor the accumulation and persistence of soluble Aβ aggregates (protofibrils and other non-fibrillar structures). Being relatively soluble in nature, such aggregates can be transported across different brain compartments, including the vasculature, where they can fibrillize if encountered by supraphysiologic concentrations of monomeric Aβ42 and Aβ40. This model supports a critical role for Aβ42 role in initiating and accelerating Aβ40 fibrillization in the vasculature, as has also been reported (19, 73).

Fibrillogenesis of Aβ Contributes to Aβ Neurotoxicity—To establish the neurotoxic activities of individual and mixed Aβ

(Aβ40 and Aβ42) monomers and aggregates, we treated cultured neurons with defined aggregate states of Aβ42 (protofibrils and fibrils) with or without the addition of monomeric Aβ (Aβ40 or Aβ42). Comparative analysis of NeuN positivity revealed that neither monomeric Aβ (Aβ40 or Aβ42) nor aggregated Aβ42 (protofibrillar or fibrillar) was sufficient to impair neuronal viability at lower (0.1 and 5 μM) concentrations (Fig. 7*A* and supplemental Fig. 6). Furthermore, adding monomeric Aβ40 to Aβ42 (monomeric, protofibrillar, or fibrillar; 5 μM each) did not enhance Aβ toxicity (Fig. 7, *A* and *D*). However, the addition of monomeric Aβ42 to protofibrillar Aβ42 (5 μM each) or 10 μM monomeric Aβ42 significantly impaired neuronal viability (Fig. 7, *A*, *C*, and *E*), suggesting that perpetuating the aggregation of Aβ42 increases Aβ toxicity. Interestingly, a higher concentration (10 μM) of protofibrillar Aβ42 or preformed Aβ42 fibrils did not show comparable toxicity (Fig. 7, *A* and *G*). These data are consistent with a dominant role for Aβ42 in impairing neuron viability (19, 25) and further implicate the ongoing Aβ self-assembly process (rather than any specific Aβ aggregation state) in Aβ-associated toxicity (51, 74). These results also add credence to therapeutic strategies aimed at disrupting the nucleation or elongation of amyloid fibrils to inhibit Aβ neurotoxicity in AD.

Conclusions—Potential interactions between Aβ40 and Aβ42 have been investigated previously by various research groups. These studies have shown that Aβ40 can inhibit the aggregation and fibril formation of Aβ42 (38, 41) and protect cultured neurons from Aβ-induced neurotoxicity (40). In addition to confirming the findings of these studies, the present study serves as a critical contribution to the current understanding of Aβ40 and Aβ42 interactions by examining the specific interplay of biophysically defined Aβ species (and mixtures thereof). Unlike previous studies suggesting that Aβ40 blocks the aggregation of monomeric Aβ42 (41), our results show that Aβ40 does not prevent further aggregation of the various Aβ42 quaternary structures (monomeric, protofibrillar, and fibrillar). Instead, we have demonstrated that Aβ40 alters the kinetic stability, solubility, and morphological properties of Aβ42 aggregates and prevents the formation of mature fibrils. Accordingly, we found that Aβ40 inhibits fibril formation of monomeric Aβ42 in a concentration-dependent manner (Fig. 1), whereas the effect on protofibril and fibril elongation is concentration-independent (Fig. 2). We have also shown that changes induced by Aβ40 are reversible upon reintroduction of high concentrations of Aβ42. Our results also confirm previous findings on the seeding capacity of Aβ40 and Aβ42 fibrils (Fig. 5), but to our knowledge this is the first report showing that Aβ42 protofibrils have the capacity to enhance the fibrillogenesis of Aβ42 but not of Aβ40 (Fig. 6*D*). Importantly, we have also begun to establish the relevance of the interactions of specific Aβ species *in vivo*. These results suggest that the continued pursuit of a quantitative and structural understanding of how Aβ40 and Aβ42 interact may eventually provide better biomarkers and therapies for the treatment of AD.

Acknowledgment—We thank Muriel Arimon for reviewing the manuscript draft and offering helpful suggestions.

REFERENCES

1. Glenner, G. G., Wong, C. W., Quaranta, V., and Eanes, E. D. (1984) *Appl. Pathol.* **2,** 357–369
2. Braak, H., and Braak, E. (1991) *Acta Neuropathol.* **82,** 239–259
3. Dickson, D. W. (1997) *J. Neuropathol. Exp. Neurol.* **56,** 321–339
4. Anderton, B. H., Callahan, L., Coleman, P., Davies, P., Flood, D., Jicha, G. A., Ohm, T., and Weaver, C. (1998) *Prog. Neurobiol.* (*Oxf.*) **55,** 595–609
5. Selkoe, D. J. (1991) *Sci. Am.* **265,** 68–71, 78
6. Yankner, B. A. (1996) *Nat. Med.* **2,** 850–852
7. Hardy, J. A., and Higgins, G. A. (1992) *Science* **256,** 184–185
8. Busciglio, J., Gabuzda, D. H., Matsudaira, P., and Yankner, B. A. (1993) *Proc. Natl. Acad. Sci. U. S. A.* **90,** 2092–2096
9. Shoji, M., Golde, T. E., Ghiso, J., Cheung, T. T., Estus, S., Shaffer, L. M., Cai, X. D., McKay, D. M., Tintner, R., and Frangione, B. (1992) *Science* **258,** 126–129
10. Haass, C., Schlossmacher, M. G., Hung, A. Y., Vigo-Pelfrey, C., Mellon, A., Ostaszewski, B. L., Lieberburg, I., Koo, E. H., Schenk, D., and Teplow, D. B. (1992) *Nature* **359,** 322–325
11. Selkoe, D. J. (1991) *Neuron* **6,** 487–498
12. Klafki, H., Abramowski, D., Swoboda, R., Paganetti, P. A., and Staufenbiel, M. (1996) *J. Biol. Chem.* **271,** 28655–28659
13. Seubert, P., Vigo-Pelfrey, C., Esch, F., Lee, M., Dovey, H., Davis, D., Sinha, S., Schiossmacher, M., Whaley, T., Swindlehurst, C., McCormack, R., Wolfert, R., Selkoe, D., Lieberburg, I., and Schenk, D. (1992) *Nature* **359,** 325–327
14. Bibl, M., Mollenhauer, B., Esselmann, H., Lewczuk, P., Trenkwalder, C., Brechlin, P., Ruther, E., Kornhuber, J., Otto, M., and Wiltfang, J. (2006) *J. Neural Transm.* **113,** 1771–1778
15. Jensen, M., Schroder, J., Blomberg, M., Engvall, B., Pantel, J., Ida, N., Basun, H., Wahlund, L. O., Werle, E., Jauss, M., Beyreuther, K., Lannfelt, L., and Hartmann, T. (1999) *Ann. Neurol.* **45,** 504–511
16. Lue, L. F., Kuo, Y. M., Roher, A. E., Brachova, L., Shen, Y., Sue, L., Beach, T., Kurth, J. H., Rydel, R. E., and Rogers, J. (1999) *Am. J. Pathol.* **155,** 853–862
17. Iwatsubo, T., Odaka, A., Suzuki, N., Mizusawa, H., Nukina, N., and Ihara, Y. (1994) *Neuron* **13,** 45–53
18. Gravina, S. A., Ho, L., Eckman, C. B., Long, K. E., Otvos, L., Jr., Younkin, L. H., Suzuki, N., and Younkin, S. G. (1995) *J. Biol. Chem.* **270,** 7013–7016
19. McGowan, E., Pickford, F., Kim, J., Onstead, L., Eriksen, J., Yu, C., Skipper, L., Murphy, M. P., Beard, J., Das, P., Jansen, K., Delucia, M., Lin, W. L., Dolios, G., Wang, R., Eckman, C. B., Dickson, D. W., Hutton, M., Hardy, J., and Golde, T. (2005) *Neuron* **47,** 191–199
20. Tamaoka, A., Kondo, T., Odaka, A., Sahara, N., Sawamura, N., Ozawa, K., Suzuki, N., Shoji, S., and Mori, H. (1994) *Biochem. Biophys. Res. Commun.* **205,** 834–842
21. Burdick, D., Soreghan, B., Kwon, M., Kosmoski, J., Knauer, M., Henschen, A., Yates, J., Cotman, C., and Glabe, C. (1992) *J. Biol. Chem.* **267,** 546–554
22. Jarrett, J. T., Berger, E. P., and Lansbury, P. T., Jr. (1993) *Biochemistry* **32,** 4693–4697
23. Jarrett, J. T., and Lansbury, P. T., Jr. (1993) *Cell* **73,** 1055–1058
24. Dahlgren, K. N., Manelli, A. M., Stine, W. B., Jr., Baker, L. K., Krafft, G. A., and LaDu, M. J. (2002) *J. Biol. Chem.* **277,** 32046–32053
25. Younkin, S. G. (1995) *Ann. Neurol.* **37,** 287–288
26. Selkoe, D. J. (2001) *Physiol. Rev.* **81,** 741–766
27. Hardy, J. (1997) *Proc. Natl. Acad. Sci. U. S. A.* **94,** 2095–2097
28. Borchelt, D. R., Thinakaran, G., Eckman, C. B., Lee, M. K., Davenport, F., Ratovitsky, T., Prada, C. M., Kim, G., Seekins, S., Yager, D., Slunt, H. H., Wang, R., Seeger, M., Levey, A. I., Gandy, S. E., Copeland, N. G., Jenkins, N. A., Price, D. L., Younkin, S. G., and Sisodia, S. S. (1996) *Neuron* **17,** 1005–1013
29. Citron, M., Westaway, D., Xia, W., Carlson, G., Diehl, T., Levesque, G., Johnson-Wood, K., Lee, M., Seubert, P., Davis, A., Kholodenko, D., Motter, R., Sherrington, R., Perry, B., Yao, H., Strome, R., Lieberburg, I., Rommens, J., Kim, S., Schenk, D., Fraser, P., St George Hyslop, P., and Selkoe, D. J. (1997) *Nat. Med.* **3,** 67–72
30. Sherrington, R., Rogaev, E. I., Liang, Y., Rogaeva, E. A., Levesque, G., Ikeda, M., Chi, H., Lin, C., Li, G., and Holman, K. (1995) *Nature* **375,** 754–760
31. Shoji, M., Matsubara, E., Kanai, M., Watanabe, M., Nakamura, T., Tomidokoro, Y., Shizuka, M., Wakabayashi, K., Igeta, Y., Ikeda, Y., Mi-

zushima, K., Amari, M., Ishiguro, K., Kawarabayashi, T., Harigaya, Y., Okamoto, K., and Hirai, S. (1998) *J. Neurol. Sci.* **158,** 134–140
32. Bibl, M., Mollenhauer, B., Esselmann, H., Lewczuk, P., Klafki, H. W., Sparbier, K., Smirnov, A., Cepek, L., Trenkwalder, C., Ruther, E., Kornhuber, J., Otto, M., and Wiltfang, J. (2006) *Brain* **129,** 1177–1187
33. Wiltfang, J., Esselmann, H., Bibl, M., Hull, M., Hampel, H., Kessler, H., Frolich, L., Schroder, J., Peters, O., Jessen, F., Luckhaus, C., Perneczky, R., Jahn, H., Fiszer, M., Maler, J. M., Zimmermann, R., Bruckmoser, R., Kornhuber, J., and Lewczuk, P. (2007) *J. Neurochem.* **101,** 1053–1059
34. Joachim, C. L., Morris, J. H., and Selkoe, D. J. (1988) *Ann. Neurol.* **24,** 50–56
35. Miller, D. L., Papayannopoulos, I. A., Styles, J., Bobin, S. A., Lin, Y. Y., Biemann, K., and Iqbal, K. (1993) *Arch. Biochem. Biophys.* **301,** 41–52
36. Herzig, M. C., Winkler, D. T., Burgermeister, P., Pfeifer, M., Kohler, E., Schmidt, S. D., Danner, S., Abramowski, D., Sturchler-Pierrat, C., Burki, K., van Duinen, S. G., Maat-Schieman, M. L., Staufenbiel, M., Mathews, P. M., and Jucker, M. (2004) *Nat. Neurosci.* **7,** 954–960
37. Kim, J., Onstead, L., Randle, S., Price, R., Smithson, L., Zwizinski, C., Dickson, D. W., Golde, T., and McGowan, E. (2007) *J. Neurosci.* **27,** 627–633
38. Hasegawa, K., Yamaguchi, I., Omata, S., Gejyo, F., and Naiki, H. (1999) *Biochemistry* **38,** 15514–15521
39. Frost, D., Gorman, P. M., Yip, C. M., and Chakrabartty, A. (2003) *Eur. J. Biochem.* **270,** 654–663
40. Zou, K., Kim, D., Kakio, A., Byun, K., Gong, J. S., Kim, J., Kim, M., Sawamura, N., Nishimoto, S., Matsuzaki, K., Lee, B., Yanagisawa, K., and Michikawa, M. (2003) *J. Neurochem.* **87,** 609–619
41. Yan, Y., and Wang, C. (2007) *J. Mol. Biol.* **369,** 909–916
42. Lashuel, H. A., Hartley, D. M., Petre, B. M., Wall, J. S., Simon, M. N., Walz, T., and Lansbury, P. T., Jr. (2003) *J. Mol. Biol.* **332,** 795–808
43. Pace, C. N., Vajdos, F., Fee, L., Grimsley, G., and Gray, T. (1995) *Protein Sci.* **4,** 2411–2423
44. Zala, D., Benchoua, A., Brouillet, E., Perrin, V., Gaillard, M. C., Zurn, A. D., Aebischer, P., and Deglon, N. (2005) *Neurobiol. Dis.* **20,** 785–798
45. Blow, D. M., Chayen, N. E., Lloyd, L. F., and Saridakis, E. (1994) *Protein Sci* **3,** 1638–1643
46. Harper, J. D., and Lansbury, P. T., Jr. (1997) *Annu. Rev. Biochem.* **66,** 385–407
47. Kodali, R., and Wetzel, R. (2007) *Curr. Opin. Struct. Biol.* **17,** 48–57
48. O'Nuallain, B., Williams, A. D., Westermark, P., and Wetzel, R. (2004) *J. Biol. Chem.* **279,** 17490–17499
49. Krebs, M. R., Morozova-Roche, L. A., Daniel, K., Robinson, C. V., and Dobson, C. M. (2004) *Protein Sci.* **13,** 1933–1938
50. DePace, A. H., and Weissman, J. S. (2002) *Nat. Struct. Biol.* **9,** 389–396
51. Wogulis, M., Wright, S., Cunningham, D., Chilcote, T., Powell, K., and Rydel, R. E. (2005) *J. Neurosci.* **25,** 1071–1080
52. Cupers, P., Bentahir, M., Craessaerts, K., Orlans, I., Vanderstichele, H., Saftig, P., De Strooper, B., and Annaert, W. (2001) *J. Cell Biol.* **154,** 731–740
53. Mucke, L., Masliah, E., Yu, G. Q., Mallory, M., Rockenstein, E. M., Tatsuno, G., Hu, K., Kholodenko, D., Johnson-Wood, K., and McConlogue, L. (2000) *J. Neurosci.* **20,** 4050–4058
54. Lemere, C. A., Lopera, F., Kosik, K. S., Lendon, C. L., Ossa, J., Saido, T. C., Yamaguchi, H., Ruiz, A., Martinez, A., Madrigal, L., Hincapie, L., Arango, J. C., Anthony, D. C., Koo, E. H., Goate, A. M., Selkoe, D. J., and Arango, J. C. (1996) *Nat. Med.* **2,** 1146–1150
55. Hsia, A. Y., Masliah, E., McConlogue, L., Yu, G. Q., Tatsuno, G., Hu, K., Kholodenko, D., Malenka, R. C., Nicoll, R. A., and Mucke, L. (1999) *Proc. Natl. Acad. Sci. U. S. A.* **96,** 3228–3233
56. Collins, S. R., Douglass, A., Vale, R. D., and Weissman, J. S. (2004) *PLoS Biol.* **2,** e321
57. Nichols, M. R., Moss, M. A., Reed, D. K., Lin, W. L., Mukhopadhyay, R., Hoh, J. H., and Rosenberry, T. L. (2002) *Biochemistry* **41,** 6115–6127
58. Lomakin, A., Teplow, D. B., Kirschner, D. A., and Benedek, G. B. (1997) *Proc. Natl. Acad. Sci. U. S. A.* **94,** 7942–7947
59. Esler, W. P., Stimson, E. R., Jennings, J. M., Vinters, H. V., Ghilardi, J. R., Lee, J. P., Mantyh, P. W., and Maggio, J. E. (2000) *Biochemistry* **39,** 6288–6295
60. Carulla, N., Caddy, G. L., Hall, D. R., Zurdo, J., Gairi, M., Feliz, M., Giralt, E., Robinson, C. V., and Dobson, C. M. (2005) *Nature* **436,** 554–558
61. O'Nuallain, B., Shivaprasad, S., Kheterpal, I., and Wetzel, R. (2005) *Biochemistry* **44,** 12709–12718
62. Walsh, D. M., Lomakin, A., Benedek, G. B., Condron, M. M., and Teplow, D. B. (1997) *J. Biol. Chem.* **272,** 22364–22372
63. Walsh, D. M., Klyubin, I., Shankar, G. M., Townsend, M., Fadeeva, J. V., Betts, V., Podlisny, M. B., Cleary, J. P., Ashe, K. H., Rowan, M. J., and Selkoe, D. J. (2005) *Biochem. Soc. Trans.* **33,** 1087–1090
64. Hartley, D. M., Walsh, D. M., Ye, C. P., Diehl, T., Vasquez, S., Vassilev, P. M., Teplow, D. B., and Selkoe, D. J. (1999) *J. Neurosci.* **19,** 8876–8884
65. Walsh, D. M., Hartley, D. M., Kusumoto, Y., Fezoui, Y., Condron, M. M., Lomakin, A., Benedek, G. B., Selkoe, D. J., and Teplow, D. B. (1999) *J. Biol. Chem.* **274,** 25945–25952
66. Walsh, D. M., Klyubin, I., Fadeeva, J. V., Cullen, W. K., Anwyl, R., Wolfe, M. S., Rowan, M. J., and Selkoe, D. J. (2002) *Nature* **416,** 535–539
67. Lambert, M. P., Barlow, A. K., Chromy, B. A., Edwards, C., Freed, R., Liosatos, M., Morgan, T. E., Rozovsky, I., Trommer, B., Viola, K. L., Wals, P., Zhang, C., Finch, C. E., Krafft, G. A., and Klein, W. L. (1998) *Proc. Natl. Acad. Sci. U. S. A.* **95,** 6448–6453
68. Lashuel, H. A., Petre, B. M., Wall, J., Simon, M., Nowak, R. J., Walz, T., and Lansbury, P. T., Jr. (2002) *J. Mol. Biol.* **322,** 1089–1102
69. Lashuel, H. A., Hartley, D., Petre, B. M., Walz, T., and Lansbury, P. T., Jr. (2002) *Nature* **418,** 291
70. Arispe, N., Rojas, E., and Pollard, H. B. (1993) *Proc. Natl. Acad. Sci. U. S. A.* **90,** 567–571
71. Caughey, B., and Lansbury, P. T. (2003) *Annu. Rev. Neurosci.* **26,** 267–298
72. Cheng, I. H., Scearce-Levie, K., Legleiter, J., Palop, J. J., Gerstein, H., Bien-Ly, N., Puolivali, J., Lesne, S., Ashe, K. H., Muchowski, P. J., and Mucke, L. (2007) *J. Biol. Chem.* **282,** 23818–23828
73. Iwatsubo, T., Mann, D. M., Odaka, A., Suzuki, N., and Ihara, Y. (1995) *Ann. Neurol.* **37,** 294–299
74. Lorenzo, A., and Yankner, B. A. (1994) *Proc. Natl. Acad. Sci. U. S. A.* **91,** 12243–12247